Why Breakup of Photons and Pions into Forward Dijets Is so Different: Predictions from Nonlinear Nuclear $k_\perp$-factorization

N.N. Nikolaev,[1,2] W. Schäfer,[1] B.G. Zakharov,[2] and V.R. Zoller[3]

[1]*IKP, Forschungszentrum Jülich, D-52425 Jülich, Germany*

[2]*L.D. Landau Institute for Theoretical Physics, Chernogolovka, Russia*

[3]*Institute for Experimental and Theoretical Physics, Moscow, Russia*

Based on an approach to non-Abelian propagation of color dipoles in a nuclear medium we formulate a nonlinear $k_\perp$-factorization for the breakup of photons and pions into forward hard dijets in terms of the collective Weizsäcker-Williams (WW) glue of nuclei. We find quite distinct practical consequences of nonlinear nuclear $k_\perp$-factorization for interactions of pointlike photons and non-pointlike pions. In the former case the large transverse momentum $p_\perp$ of jets comes from the intrinsic momentum of quarks and antiquarks in the photon and nuclear effects manifest themselves as an azimuthal decorrelation with an acoplanarity momentum of the order of the nuclear saturation momentum Q_A. In the breakup of pions off free nucleons to the leading order in pQCD the spectator parton has a small transverse momentum and the hard dijet cross section is suppressed. In the breakup of pions off heavy nuclei the forward hard jets are predicted to be entirely decorrelated. We comment on the sensitivity of the pionic dijet cross section to the pion distribution amplitude. The predicted distinction between the breakup of photons and pions can be tested by the sphericity and thrust analysis of the forward hadronic system in the COMPASS experiment at CERN.

INTRODUCTION

The trademark of the conventional perturbative QCD (pQCD) factorization theorems for hard interactions of leptons and hadrons is that the hard scattering observables are linear functionals of the appropriate parton densities in the projectile and target [1]. In contrast to that, from the parton model point of view the opacity of heavy nuclei to high energy projectiles entails a highly nonlinear relationship between the parton densities of free nucleons and nuclei. In deep inelastic scattering (DIS) off nuclei there emerges a new large scale - the nuclear saturation scale Q_A, - which separates the opaque nucleus, i.e., nonlinear, and weak attenuation, i.e., linear, regimes [2–5]. A priori it is not obvious that in the nonlinear regime with the large saturation scale one can define nuclear parton densities such that they enter different observables in a universal manner, i.e., if useful factorization theorems can be formulated for hard phenomena in ultrarelativistic heavy ion collisions. In our previous work [6, 7] we presented a partial solution to this problem - a nonlinear nuclear $k_\perp$-factorization for the production of forward hard dijets in DIS off nuclei.

The salient feature of hard dijets in deep inelastic scattering (DIS) and real photoabsorption is that the large transverse momentum $p_\perp$ of forward jets comes from the intrinsic momentum of quarks and antiquarks in the (virtual) photon. In the $k_\perp$-factorization description of the underlying photon-gluon fusion parton subprocess $\gamma^* g \to q\bar{q}$, valid at small x, the disparity of the quark and antiquark transverse momenta and departure from the exact back-to-back configuration - the acoplanarity momentum - is caused by the transverse momentum κ of gluons. It can be quantified in terms of the unintegrated gluon density of the target (see [8, 9] and references therein). Our nonlinear $k_\perp$-factorization for breakup of photons into dijets on nuclei gives a coherent description of the nuclear mass number dependence of the dijet inclusive cross section in terms of the collective Weizsäcker-Williams (WW) unintegrated nuclear glue. This WW nuclear glue has the form of an expansion over the collective gluon structure function of spatially overlapping nucleons [10] of the Lorentz-contracted ultrarelativistic nucleus [5, 11]. Apart from the case of minijets with the $p_\perp$ comparable to or below the saturation scale Q_A the principal nuclear effect is a broadening of the acoplanarity momentum distribution, and in [6] we showed how this broadening can be calculated through the collective WW nuclear unintegrated gluon density.

The breakup of pions into forward dijets in inelastic πA collisions is an excitation of the quark-antiquark Fock states of the pion. The intrinsic momentum of quarks in the non-pointlike pion is limited. To the leading order in pQCD the breakup of the pion goes via the pQCD analogue of the electrodisintegration of the deuteron (for the review see [12]), i.e., the subprocess $\pi g \to q\bar{q}$ in which the struck parton carries the transverse momentum of the absorbed gluon and the spectator parton emerges in the final state with the small transverse momentum it had in the pion, fig. 1. On the other hand, multiple gluon exchange in collisions with opaque nuclei can give a large transverse kick to both partons. In this communication we report the nonlinear nuclear $k_\perp$-factorization formulas for the breakup of pions into forward hard dijets off nuclei. One of our central results is the prediction of a complete azimuthal decorrelation of forward hard dijets.

At the parton level the produced forward jets retain the fraction $z_\pm$ of the lightcone momentum of the pion they carried in the incident pion. One may wonder whether the jet longitudinal momentum distributions would give a handle on the so-called pion distribution amplitude (πDA) [13] which with some reservations about large higher twist and next-to-leading order pQCD corrections was indeed the case in the coherent diffractive breakup of pions into djets off nuclei [11, 14, 15]. Our analysis of nonlinear nuclear $k_\perp$-factorization formulas shows that these expectations are indeed met by the contribution to the dijet inclusive cross section from the in-volume absorption of pions, which comes from the perturbatively small $q\bar{q}$ dipole states of the pion. However, this contribution is overwhelmed by a large contribution from soft absorption of large $q\bar{q}$ dipole states of the pion on the front face of a nucleus. In this case there emerges some infrared-sensitive modulation of the z-dependence of the πDA which brings a model-dependence into tests of the pion wave function (WF).

The further presentation is organized as follows. The major thrust is on the distinction between breakup of pointlike photons and non-pointlike pions. To make the discussion self-contained we present the basic formalism to a sufficient detail. In section 2 we set up the formalism with a brief discussion of the decorrelation of jets in DIS and πN scattering off free nucleons. In section 3 we present the color-dipole S-matrix formalism for the breakup into dijets on nuclear targets. In section 4 we formulate a nonlinear nuclear $k_\perp$-factorization for the inclusive dijet cross section in terms of the collective WW unintegrated gluon density of the nucleus and comment on the salient features of dijet production in DIS off nuclei. The subject of section 5 is the breakup of non-pointlike pions into dijets. In contrast to the breakup of pointlike photons in DIS, excitation of two hard jets from pions is only possible on heavy nuclei. The most striking difference from DIS and real photoproduction is that the two pionic forward hard jets produced off a nucleus are completely azimuthally decorrelated. This leading contribution to the breakup cross section comes from soft absorption of pions on the front face of a nucleus. The hard contribution from the in-volume breakup gives rise to back-to-back dijets as in DIS and has the form of a higher twist correction. Its isolation is a challenging but not impossible task and would allow the determination of the πDA. In the Conclusions we summarize our principal findings and comment on possible experimental tests of our predictions. The predicted distinction between breakup of photons and pions can tested by the sphericity and thrust analysis of the forward hadronic system in the COMPASS experiment at CERN [16].

1. FORWARD DIJETS OFF FREE NUCLEONS AND UNINTEGRATED GLUE OF THE NUCLEON

We set up the formalism on an example of breakup into dijets off free nucleons. Production of high-mass forward hard dijets selects excitation of the $q\bar{q}$ Fock states of the projectile photon and meson. The relevant pQCD diagrams are shown in figs. 1a-1d. In the color dipole approach [17–24] the fundamental quantity is the total cross section for interaction of the color dipole $\boldsymbol{r}$ with the target nucleon

$$\begin{aligned}\sigma(x,\boldsymbol{r}) &= \alpha_S(r)\sigma_0(x)\int d^2\boldsymbol{\kappa} f(\boldsymbol{\kappa})\left[1-\exp(i\boldsymbol{\kappa}\boldsymbol{r})\right]\\ &= \frac{1}{2}\alpha_S(r)\sigma_0(x)\int d^2\boldsymbol{\kappa} f(\boldsymbol{\kappa})\left[1-\exp(i\boldsymbol{\kappa}\boldsymbol{r})\right]\cdot\left[1-\exp(-i\boldsymbol{\kappa}\boldsymbol{r})\right]\,,\end{aligned} \tag{1}$$

where $f(\boldsymbol{\kappa})$ is normalized as $\int d^2\boldsymbol{\kappa} f(\boldsymbol{\kappa}) = 1$ and is related to the so-called Fadin-Kuraev-Lipatov unintegrated gluon density ([25], for the recent review and phenomenology see [26, 27]) of the target nucleon $\mathcal{F}(x,\kappa^2) = \partial G(x,\kappa^2)/\partial\log\kappa^2$ by

$$f(\boldsymbol{\kappa}) = \frac{4\pi}{N_c\sigma_0(x)}\cdot\frac{1}{\kappa^4}\cdot\mathcal{F}(x,\kappa^2)\,. \tag{2}$$

Here $\sigma_0(x)$ is an auxiliary soft parameter which drops out from major nuclear observables.

First we consider DIS where the perturbative small size of dipoles is set by the large virtuality Q^2 of the photon, and then comment how the results extend to breakup of real photons and pions into hard dijets. The total photoabsorption cross section equals

$$\sigma_N(Q^2,x) = \int d^2\boldsymbol{r} dz|\Psi(Q^2,z,\boldsymbol{r})|^2\sigma(\boldsymbol{r})\,, \tag{3}$$

where $\Psi(Q^2, z, \boldsymbol{r}) = \langle z, \boldsymbol{r}|\gamma^*\rangle$ is the WF of the $q\bar{q}$ Fock state of the photon, here-below we suppress the argument Q^2 in $\Psi(Q^2, z, \boldsymbol{r})$. Upon the relevant Fourier transformations one finds the momentum spectrum of the final state (FS) quark prior the hadronization

$$\frac{d\sigma_N}{d^2\boldsymbol{p}_+ dz} = \frac{\sigma_0(x)}{2} \cdot \frac{\alpha_S(\boldsymbol{p}_+^2)}{(2\pi)^2} \int d^2\boldsymbol{\kappa} f(\boldsymbol{\kappa}) \left|\langle\gamma^*|z, \boldsymbol{p}_+\rangle - \langle\gamma^*|z, \boldsymbol{p}_+ - \boldsymbol{\kappa}\rangle\right|^2 \tag{4}$$

where $\boldsymbol{p}_+$ is the transverse momentum of the quark jet, $\boldsymbol{p}_- = -\boldsymbol{p}_+ + \boldsymbol{\kappa}$ is the transverse momentum of the antiquark jet, $z_+ = z$ and $z_- = 1 - z$ are the fractions of the photon's lightcone momentum carried by the quark and antiquark jets, respectively. For our formalism to apply we require that the variables $z_\pm$ for the observed jets add up to unity, $x_\gamma = z_+ + z_- = 1$ and the rapidity separation of jets is small, $z_+ \sim z_- \sim 1/2$, which in the realm of DIS is often referred to as the unresolved or direct photon interaction ([28] and references therein).

Now notice that the transverse momentum of the gluon is precisely the decorrelation momentum $\boldsymbol{\Delta} = \boldsymbol{p}_+ + \boldsymbol{p}_-$ so that in the still further differential form

$$\begin{aligned}\frac{d\sigma_N}{dz d^2\boldsymbol{p}_+ d^2\boldsymbol{\Delta}} &= \frac{\sigma_0(x)}{2} \cdot \frac{\alpha_S(\boldsymbol{p}^2)}{(2\pi)^2} f(\boldsymbol{\Delta}) \left|\langle\gamma^*|z, \boldsymbol{p}_+\rangle - \langle\gamma^*|z, \boldsymbol{p}_+ - \boldsymbol{\Delta}\rangle\right|^2 \\ &= \frac{\alpha_S(\boldsymbol{p}^2)}{2\pi N_c} \cdot \frac{\mathcal{F}(x, \boldsymbol{\Delta}^2)}{\Delta^4} \cdot \left|\langle\gamma^*|z, \boldsymbol{p}_+\rangle - \langle\gamma^*|z, \boldsymbol{p}_+ - \boldsymbol{\Delta}\rangle\right|^2 .\end{aligned} \tag{5}$$

This is the leading order result from $k_\perp$-factorization, for the applications to DIS off free nucleons see [8, 9] and references therein. Upon summing over the helicities $\lambda, \overline{\lambda}$ of the final state quark and antiquark, for transverse photons and flavor f one has

$$\begin{aligned}&\left|\langle\gamma^*|z, \boldsymbol{p}\rangle - \langle\gamma^*|z, \boldsymbol{p} - \boldsymbol{\kappa}\rangle\right|^2_{\lambda_\gamma = \pm 1} = \\ &2N_c e_f^2 \alpha_{em} \left\{ [z^2 + (1-z)^2] \left(\frac{\boldsymbol{p}}{\boldsymbol{p}^2 + \varepsilon^2} - \frac{\boldsymbol{p} - \boldsymbol{\kappa}}{(\boldsymbol{p} - \boldsymbol{\kappa})^2 + \varepsilon^2} \right)^2_{\lambda + \overline{\lambda} = 0} \right. \\ &\left. + m_f^2 \left(\frac{1}{\boldsymbol{p}^2 + \varepsilon^2} - \frac{1}{(\boldsymbol{p} - \boldsymbol{\kappa})^2 + \varepsilon^2} \right)^2_{\lambda + \overline{\lambda} = \lambda_\gamma} \right\}\end{aligned} \tag{6}$$

and for longitudinal photons

$$\begin{aligned}&\left|\langle\gamma^*|z, \boldsymbol{p}\rangle - \langle\gamma^*|z, \boldsymbol{p} - \boldsymbol{\kappa}\rangle\right|^2_{\lambda_\gamma = 0} = \\ &8N_c e_f^2 \alpha_{em} Q^2 z^2 (1-z)^2 \left(\frac{1}{\boldsymbol{p}^2 + \varepsilon^2} - \frac{1}{(\boldsymbol{p} - \boldsymbol{\kappa})^2 + \varepsilon^2} \right)^2_{\lambda + \overline{\lambda} = \lambda_\gamma} ,\end{aligned} \tag{7}$$

where

$$\varepsilon^2 = z(1-z)Q^2 + m_f^2 . \tag{8}$$

The leading $\log Q^2$ contribution to the dijet cross section comes from $\boldsymbol{\Delta}^2 \lesssim \boldsymbol{p}_+^2 + \varepsilon^2$. A useful small-$\boldsymbol{\Delta}$ expansion for excitation of hard, $\boldsymbol{p}_+^2 \gg \varepsilon^2 = z(1-z)Q^2$, light flavor dijets from transverse photons is

$$\begin{aligned} \frac{d\sigma_N}{dz d^2\boldsymbol{p}_+ d^2\boldsymbol{\Delta}} &\approx \frac{1}{\pi} e_f^2 \alpha_{em} \alpha_S(\boldsymbol{p}_+^2) \left[z^2 + (1-z)^2\right] \\ &\times \frac{1}{\Delta^4} \cdot \frac{\partial G(x, \boldsymbol{\Delta}^2)}{\partial \log \boldsymbol{\Delta}^2} \cdot \frac{\boldsymbol{\Delta}^2}{(\varepsilon^2 + \boldsymbol{p}_+^2)^2} \,. \end{aligned} \tag{9}$$

Then the single-jet cross section is proportional to the logarithmic integral

$$\frac{1}{\pi} \int_0^\pi d\phi \int^{\boldsymbol{p}_+^2} \frac{d\boldsymbol{\Delta}^2}{\boldsymbol{\Delta}^2} \cdot \frac{\partial G(x, \boldsymbol{\Delta}^2)}{\partial \log \boldsymbol{\Delta}^2} = G(x, \boldsymbol{p}_+^2) \tag{10}$$

familiar from the conventional collinear approximation [1].

The small-x result (9) shows that for a pointlike projectile of which the photon is just a representative, the dijets acquire their large transverse momentum from the intrinsic momentum of the quark and antiquark in the WF of the projectile, hence dubbing this process a breakup of the photon into hard dijets is appropriate. The perturbative hard scale Q_h^2 for our process is set by $Q_h^2 \simeq (4\boldsymbol{p}_+^2 + Q^2)$ and unintegrated gluon density of the proton enters (8) at the Bjorken variable $x = (4\boldsymbol{p}_+^2 + Q^2)/W^2$, where W is the $\gamma^* p$ center of mass energy. On of the major findings of [6] is that the azimuthal decorrelation of dijets exhibits only a marginal dependence on Q^2, and the above presented formalism is fully applicable to real photons.

Similar formulas apply as well to non-pointlike pions. Indeed, as argued in [11], the final state interaction between the final state quark and antiquark can be neglected and the $q\bar{q}$ plane-wave approximation becomes applicable as soon as the invariant mass of the forward hard jets exceeds a typical mass scale of prominent meson resonances. As shown in [11] in the coherent diffractive breakup of pions into hard dijets at small x the diffractive amplitude is dominated by the pomeron-splitting mechanism of fig. 1f, when the quark and antiquark with small intrinsic transverse momentum in the pion simultaneously acquire large back-to-back transverse momentum from exchanged gluons [29] (for the confirmation of the dominance of the pomeron-splitting mechanism to the higher orders in pQCD see [14, 15]). The transverse momentum distribution in truly inelastic πN collisions is different. In contrast to the pointlike photons, for pions the $q\bar{q}$ WF $\langle \boldsymbol{p} | \pi \rangle$ is a soft function which decreases steeply at $\boldsymbol{p}^2 > 1/R_\pi^2$ (here R_π is the pion radius, for a review of the dominance of the soft WF and references see [30, 31]). We are interested in jets with the transverse momentum much larger than the intrinsic transverse momentum of (anti)quarks in a pion. The unitarity cuts of diagrams of fig. 1a-1d show that to the leading order in pQCD only one parton of the pion - let it be the quark - can pick up the large transverse momentum from the exchanged gluon and give rise to a hard jet in the pion fragmentation region of pion-nucleon interactions, the spectator jet retains the soft intrinsic transverse momentum the antiquark had inside the pion. Specifically, if the quark jet has a large transverse momentum $\boldsymbol{p}_+$, then $\langle\pi|z,\boldsymbol{p}_+\rangle$ can be neglected, $\boldsymbol{\Delta}\approx\boldsymbol{p}_+$ and the pion breakup cross section takes the form

$$\frac{d\sigma_{\pi N}}{dzd^2\boldsymbol{p}_+d^2\boldsymbol{p}_-} = \frac{\alpha_S(\boldsymbol{p}_+^2)}{2\pi}\cdot\frac{\mathcal{F}(x,\boldsymbol{p}_+^2)}{p_+^4}\cdot|\langle\pi|z,\boldsymbol{p}_-\rangle|^2\,. \tag{11}$$

It shows clearly how the spectator antiquark retains a small intrinsic transverse momentum it had in the incident pion, as an analogy cf. the electrodesintegration of the deuteron [12]. Evidently, excitation of two forward hard jets in πN collisions is only possible to higher orders in pQCD. In hard inelastic πA collisions the higher order pQCD contributions from multiple scatterings are enhanced by the size of the extended nuclear target and the purpose of this communication is a description of the breakup of pions into hard dijets in inelastic collisions off heavy nuclei within our nonlinear nuclear $k_\perp$-factorization formalism [6].

The minor technical difference from DIS is the change from the pointlike $\gamma^*q\bar{q}$ vertex $eA_\mu\overline{\Psi}\gamma_\mu\Psi$ to the non-pointlike $\pi q\bar{q}$ vertex $i\Gamma_\pi(M^2)\overline{\Psi}\gamma_5\Psi$. In terms of the quark and antiquark helicities $\lambda,\overline{\lambda}$ the $\pi q(\boldsymbol{k})\bar{q}(-\boldsymbol{k})$ vertex has the form ([11, 32])

$$\overline{\Psi}_\lambda(\boldsymbol{k})\gamma_5\Psi_{\bar{\lambda}}(-\boldsymbol{k}) = \frac{\lambda}{\sqrt{z(1-z)}}[m_f\delta_{\lambda-\bar{\lambda}} - \sqrt{2}\boldsymbol{k}\cdot\boldsymbol{e}_{-\lambda}\delta_{\lambda\bar{\lambda}}]\,, \tag{12}$$

where m_f is the quark mass and $\boldsymbol{e}_\lambda = \frac{1}{\sqrt{2}}(\lambda\boldsymbol{e}_x + i\boldsymbol{e}_y)$ is the familiar polarization vector for the state of helicity λ. In transitions of spin-zero pions into $q\bar{q}$ states with the sum of helicities $\lambda+\bar{\lambda}=\pm1$ the latter is compensated by the orbital momentum of quark and antiquark. In what follows we shall only need the leading twist term, $\propto\delta_{\lambda-\bar{\lambda}}$, in (12), cf. with the coherent diffractive breakup [11]. The corresponding radial WF $\Psi_\pi(z,\boldsymbol{r})$ is related to the $\pi\to\mu\nu$ decay constant F_π and the so-called πDA $\varphi_\pi(z)$ by

$$\Psi_\pi(z,\boldsymbol{r}=0) = \int\frac{d^2\boldsymbol{p}}{(2\pi)^2}\langle z,\boldsymbol{p}|\pi\rangle = \sqrt{\frac{\pi}{2N_c}}F_\pi\varphi_\pi(z)\,. \tag{13}$$

For the purposes of our discussion a convenient normalization is $\int_0^1 dz\,\varphi_\pi(z) = 1$. We follow the Particle Data Group convention $F_\pi = 131$ MeV [33]. The πDA depends [13] on the hard scale not shown in (13), we shall comment on the relevant scale whenever appropriate.

2. THE COLOR-DIPOLE S-MATRIX TREATMENT OF THE BREAKUP INTO DIJETS ON NUCLEAR TARGETS

We focus on the breakup into dijets at small x, $x \lesssim x_A = 1/R_A m_N \ll 1$ (R_A is the radius of the nucleus, m_N is the mass of a nucleon), when the propagation of the $q\bar{q}$ pair inside nucleus can be treated in the straight-path approximation. First we review the simpler case of DIS [6]. We work in the conventional approximation of two t-channel gluons for DIS off free nucleons. The relevant unitarity cuts of the forward Compton scattering amplitude are shown in figs. 1a-1d and describe the transition from the color-neutral $q\bar{q}$ dipole to the color-octet $q\bar{q}$ pair [1]. The unitarity cuts of the nuclear Compton scattering amplitude which correspond to the genuine inelastic DIS with color excitation of the nucleus are shown in figs. 1j,k. The diagram 1k describes multiple color excitations of a nucleus when the propagating color-octet $q\bar{q}$ pair rotates in the color space.

Let $\boldsymbol{b}_+$ and $\boldsymbol{b}_-$ be the impact parameters of the quark and antiquark, respectively, and $S_A(\{\boldsymbol{b}_j\}, \boldsymbol{b}_+, \boldsymbol{b}_-)$ be the S-matrix for interaction of the $q\bar{q}$ pair with the nucleus where $\{\boldsymbol{b}_j\}$ stands for the positions of nucleons. The initial state $|A;1\rangle$ is a color-singlet nucleus made of color-singlet nucleons and a color-singlet $q\bar{q}$ dipole, in the final state we sum over all excitations of the target nucleus when one or several nucleons have been color excited. A convenient way to sum such cross sections is offered by the closure relation [34]. Regarding the color states c_{km} of the $q_k\bar{q}_m$ pair, we sum over all octet and singlet states. Then, the 2-body inclusive spectrum is calculated in terms of the 2-body density matrix as

$$\frac{d\sigma_{inel}}{dz d^2\boldsymbol{p}_+ d^2\boldsymbol{p}_-} = \frac{1}{(2\pi)^4} \int d^2\boldsymbol{b}'_+ d^2\boldsymbol{b}'_- d^2\boldsymbol{b}_+ d^2\boldsymbol{b}_- \exp[-i\boldsymbol{p}_+(\boldsymbol{b}_+ - \boldsymbol{b}'_+) - i\boldsymbol{p}_-(\boldsymbol{b}_- - \boldsymbol{b}'_-)]$$
$$\times \Psi^*(z, \boldsymbol{b}'_+ - \boldsymbol{b}'_-) \Psi(z, \boldsymbol{b}_+ - \boldsymbol{b}_-)\, \Omega^{inel}(\boldsymbol{b}'_+, \boldsymbol{b}'_-, \boldsymbol{b}_+, \boldsymbol{b}_-)\,, \tag{14}$$

where the superscript *inel* refers to the truly inelastic cross section, with the contribution from diffractive processes subtracted. The projectile wave function Ψ in general carries a dependence on helicities, flavor, and for the photon, virtuality Q^2, which have not been put in evidence here. The generalized cross section operator $\Omega^{inel}(\boldsymbol{b}'_+, \boldsymbol{b}'_-, \boldsymbol{b}_+, \boldsymbol{b}_-)$ is expressed

---

[1] To be more precise, for arbitrary N_c color-excited $q\bar{q}$ pair is in the adjoint representation and quarks in fundamental representation of $SU(N_c)$, our reference to the color octet and triplet must not cause any confusion.

through the $q\bar{q}$–nucleus S–matrix as

$$\Omega^{inel}(\boldsymbol{b}'_+,\boldsymbol{b}'_-,\boldsymbol{b}_+,\boldsymbol{b}_-) = \sum_{A^*}\sum_{km}\langle 1;A|S^*_A(\{\boldsymbol{b}_j\},\boldsymbol{b}'_+,\boldsymbol{b}'_-)|A^*;c_{km}\rangle\langle c_{km};A^*|S_A(\{\boldsymbol{b}_j\},\boldsymbol{b}_+,\boldsymbol{b}_-)|A;1\rangle$$
$$-\langle 1;A|S^*_A(\{\boldsymbol{b}_j\},\boldsymbol{b}'_+,\boldsymbol{b}'_-)|A;1\rangle\langle 1;A|S_A(\{\boldsymbol{b}_j\},\boldsymbol{b}_+,\boldsymbol{b}_-)|A;1\rangle \tag{15}$$

Upon the application of closure in the sum over nuclear states, the first term in eq.(15) becomes

$$\sum_{A^*}\sum_{km}\langle A|\left\{\langle 1|S^*_A(\{\boldsymbol{b}_j\},\boldsymbol{b}'_+,\boldsymbol{b}'_-)|c_{km}\rangle\right\}|A^*\rangle\langle A^*|\{\langle c_{km}|S_A(\{\boldsymbol{b}_j\},\boldsymbol{b}_+,\boldsymbol{b}_-)|1\rangle\}|A\rangle =$$
$$= \langle A|\left\{\sum_{km}\langle 1|S^*_A(\{\boldsymbol{b}_j\},\boldsymbol{b}'_+,\boldsymbol{b}'_-)|c_{km}\rangle\langle c_{km}|S_A(\{\boldsymbol{b}_j\},\boldsymbol{b}_+,\boldsymbol{b}_-)|1\rangle\right\}|A\rangle\,, \tag{16}$$

and can be considered as an intranuclear evolution operator for the 2-body density matrix.

The further analysis of (16) is a non-Abelian generalization of the formalism developed by one of the authors (BGZ) for the in-medium evolution of ultrarelativistic positronium [35]. Let the QCD eikonal for the quark-nucleon and antiquark-nucleon one-gluon exchange interaction be $T^a_+\Delta(\boldsymbol{b})$ and $T^a_-\Delta(\boldsymbol{b})$, where T^a_+ and T^a_- are the $SU(N_c)$ generators for the quark and antiquarks states, respectively. The vertex V_a for excitation of the nucleon $g^aN \to N^*_a$ into a color octet state is so normalized that after application of closure the vertex g^ag^bNN in the diagrams of fig. 1a-d is δ_{ab}. Then, to the two-gluon exchange approximation, the S-matrix of the $(q\bar{q})$-nucleon interaction equals

$$S_N(\boldsymbol{b}_+,\boldsymbol{b}_-) = 1 + i[T^a_+\Delta(\boldsymbol{b}_+) + T^a_-\Delta(\boldsymbol{b}_-)]V_a - \frac{1}{2}[T^a_+\Delta(\boldsymbol{b}_+) + T^a_-\Delta(\boldsymbol{b}_-)]^2\,. \tag{17}$$

The profile function for interaction of the $q\bar{q}$ dipole with a nucleon is $\Gamma(\boldsymbol{b}_+,\boldsymbol{b}_-) = 1 - S_N(\boldsymbol{b}_+,\boldsymbol{b}_-)$ and the dipole cross section for color-singlet $q\bar{q}$ dipole equals

$$\sigma(\boldsymbol{b}_+ - \boldsymbol{b}_-) = 2\int d^2\boldsymbol{b}_+\langle N|\Gamma(\boldsymbol{b}_+,\boldsymbol{b}_-)|N\rangle = \frac{N_c^2-1}{2N_c}\int d^2\boldsymbol{b}_+[\Delta(\boldsymbol{b}_+) - \Delta(\boldsymbol{b}_-)]^2\,. \tag{18}$$

The nuclear S-matrix of the straight-path approximation for the dilute-gas nucleus is given by [34]

$$S_A(\{\boldsymbol{b}_j\},\boldsymbol{b}_+,\boldsymbol{b}_-) = \prod_{j=1}^{A} S_N(\boldsymbol{b}_+ - \boldsymbol{b}_j,\boldsymbol{b}_- - \boldsymbol{b}_j) \tag{19}$$

where the ordering along the longitudinal path is understood. To the two-gluon exchange approximation, only the terms quadratic in $\Delta(\boldsymbol{b}_j)$ must be kept in the evaluation of the single-nucleon matrix elements

$$\langle N_j|S^*_N(\boldsymbol{b}'_+ - \boldsymbol{b}_j,\boldsymbol{b}'_- - \boldsymbol{b}_j)S_N(\boldsymbol{b}_+ - \boldsymbol{b}_j,\boldsymbol{b}_- - \boldsymbol{b}_j)|N_j\rangle$$

which enter the calculation of $S_A^* S_A$. The evolution operator for the 2-body density matrix (16) equals the S-matrix $S_{4A}(\boldsymbol{b}_+, \boldsymbol{b}_-, \boldsymbol{b}'_+, \boldsymbol{b}'_-)$ for scattering of a fictitious 4-parton state composed of two quark-antiquark pairs in an overall color-singlet state [35–37]. Namely, because $(T_+^a)^* = -T_-^a$, within the two-gluon exchange approximation the quarks entering the complex-conjugate S_A^* in (16) can be viewed as antiquarks, so that

$$\sum_{km} \langle 1|S_A^*(\{\boldsymbol{b}_j\}, \boldsymbol{b}'_+, \boldsymbol{b}'_-)|c_{km}\rangle\langle c_{km}|S_A(\{\boldsymbol{b}_j\}, \boldsymbol{b}_+, \boldsymbol{b}_-)|1\rangle = \\ = \sum_{kmjl} \delta_{kl}\delta_{mj}\langle c_{km}c_{jl}|S_{4A}(\boldsymbol{b}'_+, \boldsymbol{b}'_-, \boldsymbol{b}_+, \boldsymbol{b}_-)|11\rangle \,. \qquad (20)$$

While the first $q\bar{q}$ pair is formed by the initial quark q and antiquark $\bar{q}$ at impact parameters $\boldsymbol{b}_+$ and $\boldsymbol{b}_-$, respectively, in the second pair $q'\bar{q}'$ the quark q' propagates at an impact parameter $\boldsymbol{b}'_-$ and the antiquark $\bar{q}'$ at an impact parameter $\boldsymbol{b}'_+$. In the initial state both the $q\bar{q}$ and $q'\bar{q}'$ pairs are in color-singlet states: $|in\rangle = |11\rangle$. The sum over color states of the produced quark-antiquark pair can be represented as

$$\sum_{km} \langle c_{km}c_{km}|S_{4A}(\boldsymbol{b}'_+, \boldsymbol{b}'_-, \boldsymbol{b}_+, \boldsymbol{b}_-)|11\rangle = \langle 11|S_{4A}(\boldsymbol{b}'_+, \boldsymbol{b}'_-, \boldsymbol{b}_+, \boldsymbol{b}_-)|11\rangle \\ + \sqrt{N_c^2 - 1}\langle 88|S_{4A}(\boldsymbol{b}'_+, \boldsymbol{b}'_-, \boldsymbol{b}_+, \boldsymbol{b}_-)|11\rangle \,. \qquad (21)$$

Let $\sigma_4(\boldsymbol{b}'_+, \boldsymbol{b}'_-, \boldsymbol{b}_+, \boldsymbol{b}_-)$ be the color-dipole cross section operator for the 4-body state. It is convenient to introduce the average impact parameter

$$\boldsymbol{b} = \frac{1}{4}(\boldsymbol{b}_+ + \boldsymbol{b}'_+ + \boldsymbol{b}_- + \boldsymbol{b}'_-) \,, \qquad (22)$$

and

$$\boldsymbol{s} = \boldsymbol{b}_+ - \boldsymbol{b}'_+ \,, \qquad (23)$$

for the variable conjugate to the decorrelation momentum, in terms of which

$$\boldsymbol{b}_+ - \boldsymbol{b}'_- = \boldsymbol{s} + \boldsymbol{r}' \,, \quad \boldsymbol{b}_- - \boldsymbol{b}'_+ = \boldsymbol{s} - \boldsymbol{r} \,, \quad \boldsymbol{b}_- - \boldsymbol{b}'_- = \boldsymbol{s} - \boldsymbol{r} + \boldsymbol{r}' \,. \qquad (24)$$

Then the standard evaluation of the nuclear expectation value for a dilute gas nucleus neglecting the size of color dipoles compared to the radius of a heavy nucleus gives [34]

$$S_{4A}(\boldsymbol{b}'_+, \boldsymbol{b}'_-, \boldsymbol{b}_+, \boldsymbol{b}_-) = \exp[-\frac{1}{2}\sigma_4(\boldsymbol{s}, \boldsymbol{r}, \boldsymbol{r}')T(\boldsymbol{b})] \qquad (25)$$

where

$$T(\boldsymbol{b}) = \int db_z n_A(b_z, \boldsymbol{b}) \qquad (26)$$

is the optical thickness of a nucleus at an impact parameter $\boldsymbol{b}$, the nuclear matter density $n_A(b_z, \boldsymbol{b})$ is so normalized that $\int db_z d^2\boldsymbol{b} n_A(z, \boldsymbol{b}) = A$. The single-nucleon S-matrix (17) contains transitions from the color-singlet to the both color-singlet and color-octet $q\bar{q}$ pairs. However, only the color-singlet operators contribute to $\langle N_j | S_N^*(\boldsymbol{b}'_+ - \boldsymbol{b}_j, \boldsymbol{b}'_- - \boldsymbol{b}_j) S_N(\boldsymbol{b}_+ - \boldsymbol{b}_j, \boldsymbol{b}_- - \boldsymbol{b}_j) | N_j \rangle$, and the matrix $\sigma_4(\boldsymbol{s}, \boldsymbol{r}, \boldsymbol{r}')$ only includes transitions between the $|11\rangle$ and $|88\rangle$ color-singlet 4-parton states.

The calculation of $\sigma_4(\boldsymbol{s}, \boldsymbol{r}, \boldsymbol{r}')$ is found in [6], here we only cite the results:

$$\sigma_{11} = \langle 11|\sigma_4|11\rangle = \sigma(\boldsymbol{r}) + \sigma(\boldsymbol{r}')\,, \tag{27}$$

$$\begin{aligned}\sigma_{88} = \langle 88|\sigma_4|88\rangle = \; & \frac{N_c^2 - 2}{N_c^2 - 1}[\sigma(\boldsymbol{s}) + \sigma(\boldsymbol{s} - \boldsymbol{r} + \boldsymbol{r}')] + \frac{2}{N_c^2 - 1}[\sigma(\boldsymbol{s} + \boldsymbol{r}') + \sigma(\boldsymbol{s} - \boldsymbol{r})] \\ & - \frac{1}{N_c^2 - 1}[\sigma(\boldsymbol{r}) + \sigma(\boldsymbol{r}')]\,,\end{aligned} \tag{28}$$

$$\begin{aligned}\sigma_{18} = \sigma_{81} = \langle 11|\sigma_4|88\rangle = \; & \frac{1}{\sqrt{N_c^2 - 1}}\,[\sigma(\boldsymbol{s}) - \sigma(\boldsymbol{s} + \boldsymbol{r}') - \sigma(\boldsymbol{s} - \boldsymbol{r}) + \sigma(\boldsymbol{s} - \boldsymbol{r} + \boldsymbol{r}')] \\ \equiv \; & -\frac{\Sigma_{18}(\boldsymbol{s}, \boldsymbol{r}, \boldsymbol{r}')}{\sqrt{N_c^2 - 1}}\,.\end{aligned} \tag{29}$$

The term in (14), which subtracts the contribution from processes without color excitation of the target nucleus, equals

$$\begin{aligned}\langle 1; A|S_A^*(\boldsymbol{b}'_+, \boldsymbol{b}'_-)|A; 1\rangle\langle 1; A|S_A(\boldsymbol{b}_+, \boldsymbol{b}_-)|A; 1\rangle \; & = \exp\{-\frac{1}{2}\,[\sigma(\boldsymbol{r}) + \sigma(\boldsymbol{r}')]\,T(\boldsymbol{b})\} \\ & = \exp[-\frac{1}{2}\sigma_{11} T(\boldsymbol{b})]\end{aligned} \tag{30}$$

It is convenient to use the Sylvester expansion

$$\exp[-\frac{1}{2}\sigma_4 T(\boldsymbol{b})] = \exp[-\frac{1}{2}\Sigma_1 T(\boldsymbol{b})]\frac{\sigma_4 - \Sigma_2}{\Sigma_1 - \Sigma_2} + \exp[-\frac{1}{2}\Sigma_2 T(\boldsymbol{b})]\frac{\sigma_4 - \Sigma_1}{\Sigma_2 - \Sigma_1} \tag{31}$$

where $\Sigma_{1,2}$ are the two eigenvalues of the operator σ_4,

$$\Sigma_{1,2} = \frac{1}{2}(\sigma_{11} + \sigma_{88}) \mp \frac{1}{2}(\sigma_{11} - \sigma_{88})\sqrt{1 + \frac{4\sigma_{18}^2}{(\sigma_{11} - \sigma_{88})^2}}\,. \tag{32}$$

An application to (21) of the Sylvester expansion gives for the function Ω^{inel} in the integrand of (14)

$$\begin{aligned}
\Omega^{inel}(\boldsymbol{b}'_+,\boldsymbol{b}'_-,\boldsymbol{b}_+,\boldsymbol{b}_-) = &\quad (\langle 11| + \sqrt{N_c^2-1}\langle 88|)\exp\left[-\frac{1}{2}\sigma_4 T(\boldsymbol{b})\right]|11\rangle - \exp\left[-\frac{1}{2}\sigma_{11}T(\boldsymbol{b})\right] \\
= &\quad \exp\left[-\frac{1}{2}\Sigma_2 T(\boldsymbol{b})\right] - \exp\left[-\frac{1}{2}\sigma_{11}T(\boldsymbol{b})\right] \\
&+\frac{\sigma_{11}-\Sigma_2}{\Sigma_1-\Sigma_2}\left\{\exp\left[-\frac{1}{2}\Sigma_1 T(\boldsymbol{b})\right] - \exp\left[-\frac{1}{2}\Sigma_2 T(\boldsymbol{b})\right]\right\} \\
&+\frac{\sqrt{N_c^2-1}\sigma_{18}}{\Sigma_1-\Sigma_2}\left\{\exp\left[-\frac{1}{2}\Sigma_1 T(\boldsymbol{b})\right] - \exp\left[-\frac{1}{2}\Sigma_2 T(\boldsymbol{b})\right]\right\}
\end{aligned} \quad (33)$$

Notice that the difference between Σ_2 and $\sigma_{11} = \sigma(\boldsymbol{r}) + \sigma(\boldsymbol{r}')$ is quadratic or higher order in the off-diagonal σ_{18}, see eq. (32). Consequently, the first two lines in the Sylvester expansion (33) start with terms $\propto \sigma_{18}^2$, whereas the last line starts with terms $\propto \sigma_{18}$. Then it is convenient to represent (33) as an impulse approximation (IA) term times a nuclear distortion factor $D_A(\boldsymbol{s},\boldsymbol{r},\boldsymbol{r}',\boldsymbol{b})$,

$$\Omega^{inel}(\boldsymbol{b}'_+,\boldsymbol{b}'_-,\boldsymbol{b}_+,\boldsymbol{b}_-) \equiv \Sigma_{18}(\boldsymbol{s},\boldsymbol{r},\boldsymbol{r}')D_A(\boldsymbol{s},\boldsymbol{r},\boldsymbol{r}',\boldsymbol{b})\,, \quad (34)$$

so that

$$\begin{aligned}
\frac{d\sigma^{inel}}{d^2\boldsymbol{b}dzd^2\boldsymbol{p}_+d^2\boldsymbol{p}_-} &= \frac{1}{2(2\pi)^4}\int d^2\boldsymbol{s}d^2\boldsymbol{r}d^2\boldsymbol{r}'\exp[-i(\boldsymbol{p}_++\boldsymbol{p}_-)\boldsymbol{s}+i\boldsymbol{p}_-(\boldsymbol{r}'-\boldsymbol{r})] \\
&\times\ \Psi^*(z,\boldsymbol{r}')\Psi(z,\boldsymbol{r})T(\boldsymbol{b})D_A(\boldsymbol{s},\boldsymbol{r},\boldsymbol{r}',\boldsymbol{b})\Sigma_{18}(\boldsymbol{s},\boldsymbol{r},\boldsymbol{r}')\,.
\end{aligned} \quad (35)$$

What we need is a Fourier representation for each and every factor in (35).

3. NONLINEAR $K_\perp$-FACTORIZATION FOR BREAKUP INTO DIJETS AND COLLECTIVE WW GLUE OF NUCLEI

Upon the application of (1) the IA factor in (17) admits the simple Fourier representation

$$\begin{aligned}
&\Sigma_{18}(\boldsymbol{s},\boldsymbol{r},\boldsymbol{r}') = \sigma(\boldsymbol{s}+\boldsymbol{r}') + \sigma(\boldsymbol{s}-\boldsymbol{r}) - \sigma(\boldsymbol{s}) - \sigma(\boldsymbol{s}-\boldsymbol{r}+\boldsymbol{r}') \\
&= \alpha_S\sigma_0(x)\int d^2\boldsymbol{\kappa}f(\boldsymbol{\kappa})\exp[i\boldsymbol{\kappa}\boldsymbol{s}]\left\{1-\exp[i\boldsymbol{\kappa}\boldsymbol{r}']\right\}\left\{1-\exp[-i\boldsymbol{\kappa}\boldsymbol{r}]\right\}\,,
\end{aligned} \quad (36)$$

The Fourier representation of the nuclear distortion factor in terms of the collective nuclear WW gluon distribution as defined in [5, 11] is not a trivial task, though, appealing analytic results are derived in the large-N_c approximation.

The crucial point is that in the large-N_c approximation $\Sigma_1 = \sigma(\boldsymbol{s}) + \sigma(\boldsymbol{s}+\boldsymbol{r}'-\boldsymbol{r})$ and $\Sigma_2 = \Sigma_{22} = \sigma(\boldsymbol{r})+\sigma(\boldsymbol{r}')$, so that only the last term in the Sylvester expansion (33) contributes to the jet-jet inclusive cross section. At large N_c the initial color singlet dipole excites to the color–octet state and further intranuclear color exchanges only rotate the dipole between different color–octet states. This is indicated schematically in fig. 2. Then the nuclear distortion factor takes on a simple form

$$D_A(\boldsymbol{s},\boldsymbol{r},\boldsymbol{r}',\boldsymbol{b}) = \frac{2}{(\Sigma_2-\Sigma_1)T(\boldsymbol{b})}\left\{\exp\left[-\frac{1}{2}\Sigma_1 T(\boldsymbol{b})\right] - \exp\left[-\frac{1}{2}\Sigma_2 T(\boldsymbol{b})\right]\right\}. \qquad (37)$$

The denominator $(\Sigma_2-\Sigma_1)$ is problematic from the point of view of the Fourier transform, but it can be eliminated by the integral representation

$$\begin{aligned} D_A(\boldsymbol{s},\boldsymbol{r},\boldsymbol{r}',\boldsymbol{b}) &= \int_0^1 d\beta \exp\left\{-\frac{1}{2}[\beta\Sigma_1+(1-\beta)\Sigma_2]T(\boldsymbol{b})\right\} = \\ &= \int_0^1 d\beta \exp\left\{-\frac{1}{2}(1-\beta)[\sigma(\boldsymbol{r})+\sigma(\boldsymbol{r}')]T(\boldsymbol{b})\right\} \\ &\times \exp\left\{-\frac{1}{2}\beta[\sigma(\boldsymbol{s})+\sigma(\boldsymbol{s}+\boldsymbol{r}'-\boldsymbol{r})]T(\boldsymbol{b})\right\}. \end{aligned} \qquad (38)$$

Here the former two exponential factors describe the initial state (IS) intranuclear distortion of the incoming color-singlet $(q\bar{q})$ dipole state, whereas the last two factors describe the FS distortion of the outgoing color-octet states.

Next we apply to the exponential factors in (38) the NSS representation in terms of the collective WW unintegrated gluon density of the nucleus [5, 11]:

$$\exp\left[-\frac{1}{2}\sigma(\boldsymbol{s})T(\boldsymbol{b})\right] = \int d^2\boldsymbol{\kappa}\Phi(\nu_A(\boldsymbol{b}),\boldsymbol{\kappa})\exp(i\boldsymbol{\kappa}\boldsymbol{s}), \qquad (39)$$

where

$$\Phi(\nu_A(\boldsymbol{b}),\boldsymbol{\kappa}) = \sum_{j\geq 0} w_j(\nu_A(\boldsymbol{b}))f^{(j)}(\boldsymbol{\kappa}) = \exp(-\nu_A(\boldsymbol{b}))f^{(0)}(\boldsymbol{\kappa}) + \phi_{WW}(\nu_A(\boldsymbol{b}),\boldsymbol{\kappa}). \qquad (40)$$

Here $\phi_{WW}(\nu_A(\boldsymbol{b}),\boldsymbol{\kappa})$ is the unintegrated collective nuclear Weizsäcker-Williams glue per unit area in the impact parameter plane,

$$w_j(\nu_A(\boldsymbol{b})) = \frac{\nu_A^j(\boldsymbol{b})}{j!}\exp\left[-\nu_A(\boldsymbol{b})\right] \qquad (41)$$

is a probability of finding j spatially overlapping nucleons at an impact parameter $\boldsymbol{b}$ in a Lorentz-contracted nucleus,

$$\nu_A(\boldsymbol{b}) = \frac{1}{2}\alpha_S(r)\sigma_0(x)T(\boldsymbol{b}), \qquad (42)$$

and

$$f^{(j)}(\boldsymbol{\kappa}) = \int \prod_{i=1}^{j} d^2\boldsymbol{\kappa}_i f(\boldsymbol{\kappa}_i)\delta(\boldsymbol{\kappa} - \sum_{i=1}^{j} \boldsymbol{\kappa}_i)\,, \quad f^{(0)}(\boldsymbol{\kappa}) = \delta(\boldsymbol{\kappa}) \tag{43}$$

is a collective gluon field of j overlapping nucleons. As shown in [5, 11] the collective nuclear unintegrated gluon density $\phi_{WW}(\nu_A(\boldsymbol{b}), \boldsymbol{\kappa})$ enters the calculation of the nuclear sea quark density in precisely the same way as $f(\boldsymbol{\kappa})$ in (5) for the free nucleon target.

We cite two important features of $\phi_{WW}(\nu_A(\boldsymbol{b}), \boldsymbol{\kappa})$. First, the hard tail of the unintegrated nuclear glue per bound nucleon is calculated parameter free [11],

$$f_{WW}(\nu_A(\boldsymbol{b}), \boldsymbol{\kappa}) = \frac{\phi_{WW}(\nu_A(\boldsymbol{b}), \boldsymbol{\kappa})}{\nu_A(\boldsymbol{b})} = f(\boldsymbol{\kappa}) \left[1 + \frac{2C_A \pi^2 \gamma^2 \alpha_S(r) T(\boldsymbol{b})}{C_F N_c \boldsymbol{\kappa}^2} G(\boldsymbol{\kappa}^2)\right]\,, \tag{44}$$

and does not depend on the infrared parameter $\sigma_0(x)$. In the hard regime the differential nuclear glue is not shadowed, furthermore, because of the manifestly positive-valued and model-independent nuclear higher twist correction it exhibits a nuclear antishadowing property [11]. Second, for interactions with nuclei of $q\bar{q}$ dipoles with $|\boldsymbol{r}| \gtrsim 1/Q_A$, the strong coupling enters (42) as $\alpha_S(Q_A^2)$ and in the saturation region of $\boldsymbol{\kappa}^2 \lesssim Q_A^2$ we have [5, 6]

$$\Phi(\nu_A(\boldsymbol{b}), \boldsymbol{\kappa}) \approx \phi_{WW}(\nu_A(\boldsymbol{b}), \boldsymbol{\kappa}) \approx \frac{1}{\pi} \frac{Q_A^2}{(\boldsymbol{\kappa}^2 + Q_A^2)^2}\,, \tag{45}$$

where the width of the plateau Q_A which is the nuclear saturation scale equals

$$Q_A^2 \approx \frac{4\pi^2}{N_c} \alpha_S(Q_A^2) G(Q_A^2) T(\boldsymbol{b}) \tag{46}$$

and exhibits only weak dependence on the infrared parameters through the Q_A^2 dependence of the running strong coupling and scaling violations in the unintegrated gluon density of the nucleon. For instance, at $x = 10^{-2}$ the numerical results [26] for $G(Q^2)$ correspond to a nearly Q^2 independent $\alpha_S(Q^2)G(Q^2) \approx 1$. For average DIS on a heavy nucleus, $A^{1/3} = 6$, we found $\langle Q_A^2(\boldsymbol{b})\rangle \approx 0.9\ (GeV/c)^2$.

Now we are in the position to represent the nuclear distortion factor (38) as

$$\begin{aligned} D_A(\boldsymbol{s}, \boldsymbol{r}, \boldsymbol{r}', \boldsymbol{b}) = \int_0^1 d\beta \quad & \int d^2\boldsymbol{\kappa}_1 \Phi((1-\beta)\nu_A(\boldsymbol{b}), \boldsymbol{\kappa}_1) \exp(-i\boldsymbol{\kappa}_1 \boldsymbol{r}) \\ \times & \int d^2\boldsymbol{\kappa}_2 \Phi((1-\beta)\nu_A(\boldsymbol{b}), \boldsymbol{\kappa}_2) \exp(i\boldsymbol{\kappa}_2 \boldsymbol{r}') \\ \times & \int d^2\boldsymbol{\kappa}_3 \Phi(\beta\nu_A(\boldsymbol{b}), \boldsymbol{\kappa}_3) \exp[i\boldsymbol{\kappa}_3(\boldsymbol{s} + \boldsymbol{r}' - \boldsymbol{r})] \\ \times & \int d^2\boldsymbol{\kappa}_4 \Phi(\beta\nu_A(\boldsymbol{b}), \boldsymbol{\kappa}_4) \exp(i\boldsymbol{\kappa}_4 \boldsymbol{s})\,, \end{aligned} \tag{47}$$

so that the jet-jet inclusive inelastic cross section takes the form

$$\frac{d\sigma_{inel}}{d^2\boldsymbol{b}dzd^2\boldsymbol{p}_-d^2\boldsymbol{\Delta}} = \frac{1}{2(2\pi)^2}\alpha_S\sigma_0(x)T(\boldsymbol{b})\int_0^1 d\beta\int d^2\boldsymbol{\kappa}_3 d^2\boldsymbol{\kappa} f(\boldsymbol{\kappa})$$
$$\times\ \Phi(\beta\nu_A(\boldsymbol{b}),\boldsymbol{\Delta}-\boldsymbol{\kappa}_3-\boldsymbol{\kappa})\Phi(\beta\nu_A(\boldsymbol{b}),\boldsymbol{\kappa}_3)$$
$$\times\left|\int d^2\boldsymbol{\kappa}_1\Phi((1-\beta)\nu_A(\boldsymbol{b}),\boldsymbol{\kappa}_1)\left\{\langle\gamma^*|z,\boldsymbol{p}_-+\boldsymbol{\kappa}_1+\boldsymbol{\kappa}_3\rangle-\langle\gamma^*|z,\boldsymbol{p}_-+\boldsymbol{\kappa}_1+\boldsymbol{\kappa}_3+\boldsymbol{\kappa}\rangle\right\}\right|^2 \quad (48)$$

The transverse momentum distribution of dijets is uniquely calculable in terms of the collective WW glue of a nucleus and as such (48) can be regarded as a nonlinear nuclear $k_\perp$-factorization for the inclusive inelastic dijet cross section. Notice that the convolution in the last line of eq. (48) describes the initial state distortion of the color singlet $q\bar{q}$–state in the projectile.

There are two important limiting cases. We start with hard dijets, $|\boldsymbol{p}_\pm| \gtrsim Q_A$. A crucial point is that the WF of the pointlike photon is a slowly decreasing function of the transverse momentum, in contrast to $\Phi(\nu_A(\boldsymbol{b}),\boldsymbol{\kappa})$ which is a steeply decreasing function, compare eqs. (6),(7) to eq. (45). Then, since $\boldsymbol{\kappa}_i^2 \lesssim Q_A^2$, for hard dijets one can neglect $\boldsymbol{\kappa}_1,\boldsymbol{\kappa}_3$ compared to $\boldsymbol{p}_\pm$ and approximate

$$\int d^2\boldsymbol{\kappa}_1\Phi((1-\beta)\nu_A(\boldsymbol{b}),\boldsymbol{\kappa}_1)\left\{\langle\gamma^*|z,\boldsymbol{p}_-+\boldsymbol{\kappa}_1+\boldsymbol{\kappa}_3\rangle-\langle\gamma^*|z,\boldsymbol{p}_-+\boldsymbol{\kappa}_1+\boldsymbol{\kappa}_3+\boldsymbol{\kappa}\rangle\right\}$$
$$\approx \langle\gamma^*|z,\boldsymbol{p}_-\rangle-\langle\gamma^*|z,\boldsymbol{p}_-+\boldsymbol{\kappa}\rangle\,,\,. \quad (49)$$

which amounts to negligible IS distortion of small color-singlet dipoles with $|\boldsymbol{r}|,|\boldsymbol{r}'| \sim 1/|\boldsymbol{p}_\pm| \lesssim 1/Q_A$. Next we notice that

$$\int d^2\boldsymbol{\kappa}_3\,\Phi(\beta\nu_A(\boldsymbol{b}),\boldsymbol{\Delta}-\boldsymbol{\kappa}_3-\boldsymbol{\kappa})\Phi(\beta\nu_A(\boldsymbol{b}),\boldsymbol{\kappa}_3) = \Phi(2\beta\nu_A(\boldsymbol{b}),\boldsymbol{\Delta}-\boldsymbol{\kappa})\,, \quad (50)$$

so that the hard jet-jet inclusive cross section takes the form

$$\frac{d\sigma_{inel}}{d^2\boldsymbol{b}dzd^2\boldsymbol{p}_+d^2\boldsymbol{\Delta}} = T(\boldsymbol{b})\int_0^1 d\beta\int d^2\boldsymbol{\kappa}\,\Phi(2\beta\nu_A(\boldsymbol{b}),\boldsymbol{\Delta}-\boldsymbol{\kappa})\frac{d\sigma_N}{dzd^2\boldsymbol{p}_+d^2\boldsymbol{\kappa}}\,, \quad (51)$$

which is a close counterpart of, but still different from, the conventional $k_\perp$-factorization (3) for the free nucleon target. As a matter of fact, for hard dijets one does not need to invoke the large–N_c approximation: here $|\boldsymbol{r}|,|\boldsymbol{r}'| \ll |\boldsymbol{s}|$, so that $\Sigma_1 \sim 0$, $\Sigma_2 \sim 2\lambda_c\sigma(\boldsymbol{s})$, where $\lambda_c = N_c^2/(N_c^2-1)$, and one can replace $\Phi(2\beta\nu_A(\boldsymbol{b}),\boldsymbol{\Delta}-\boldsymbol{\kappa})$ by $\Phi(2\lambda_c\beta\nu_A(\boldsymbol{b}),\boldsymbol{\Delta}-\boldsymbol{\kappa})$, see a discussion in [6]. All the dependence on transverse momentum p_+ of the hard jet is in the free nucleon cross section $d\sigma_N$, i.e., the pQCD treatment breakup into hard dijets is applicable to DIS on the free nucleon and nuclear targets on the same footing. The effect of the collective nuclear glue $\Phi(2\beta\nu_A(\boldsymbol{b}),\boldsymbol{\kappa})$ is a smearing/broadening as well as decorrelation of the dijets. Numerical estimates for the azimuthal decorrelation of jets and a discussion concerning the relevance to the RHIC-STAR finding [38] of the disappearance of the away jet in central $AuAu$ collisions can be found in [6]. In this hard dijet limit it is tempting to assign to $\Phi(2\beta\nu_A(\boldsymbol{b}),\boldsymbol{\kappa})$ a probabilistic interpretation as an intrinsic transverse momentum distribution of collective nuclear gluons, but this collectivization only applies to the fraction β of the nuclear thickness which the $(q\bar{q})$ pair propagates in the color octet state.

The second limiting case is that of minijets $|\boldsymbol{p}_-|, |\boldsymbol{\Delta}| \lesssim Q_A$. Since $|\boldsymbol{\kappa}_i| \sim Q_A$ one can neglect $\boldsymbol{p}_-$ in the photon's wave functions,

$$\int d^2\boldsymbol{\kappa}_1 \Phi((1-\beta)\nu_A(\boldsymbol{b}),\boldsymbol{\kappa}_1)\left\{\langle\gamma^*|z,\boldsymbol{p}_- + \boldsymbol{\kappa}_1 + \boldsymbol{\kappa}_3\rangle - \langle\gamma^*|z,\boldsymbol{p}_- + \boldsymbol{\kappa}_1 + \boldsymbol{\kappa}_3 + \boldsymbol{\kappa}\rangle\right\}$$
$$\approx |\langle\gamma^*|z,\boldsymbol{\kappa}_3\rangle - \langle\gamma^*|z,\boldsymbol{\kappa}_3 + \boldsymbol{\kappa}\rangle|^2 \,. \qquad (52)$$

The principal point is that the minijet-minijet inclusive cross section would depend neither on the minijet momentum nor on the decorrelation momentum. This proves a complete disappearance of the azimuthal correlation of minijets with a transverse momentum below the saturation scale.

4. NONLINEAR $K_\perp$-FACTORIZATION FOR THE BREAKUP OF PIONS INTO FORWARD DIJETS ON NUCLEI

4.1. *From pointlike photons to non-pointlike pions*

By requiring the production of forward dijets which satisfy the $x_\gamma = 1$ criterion we select the breakup of the $q\bar{q}$ Fock state of the projectile. Above we concentrated on the breakup of a pointlike projectile, in which case the back-to-back dijets stem from "lifting onto mass-shell" of $q\bar{q}$ states with a large intrinsic transverse momentum $\boldsymbol{p}_\perp$. In this section we go to another extreme case - the non-pointlike projectile, a pion, with a soft $q\bar{q}$ WF such that the intrinsic transverse momentum of the quark and antiquark is limited.

An important point is the rôle that unitarity plays in the isolation of truly inelastic collisions which is effected by a subtraction of the coherent diffractive components in (38). As is well known, in collisions of strongly interaction hadrons (pions) with opaque nuclei unitarity entails that coherent elastic scattering off a nucleus, $\pi A \to \pi A$, makes 50% of the total hadron-nucleus cross section. On the other hand, for weakly interacting pointlike projectiles (photons) it is coherent diffractive excitation of the continuum $q\bar{q}$ states, $\gamma^* A \to (q\bar{q})\ A$, which makes 50% of the total DIS cross section [22]. In our formalism as exposed in section 3, we explicitly associate the subtracted coherent diffractive component in (14) with the continuum $q\bar{q}$ dijets. Strictly speaking, in the case of incident pions the subtraction of coherent diffractive processes must include a sum over elastic pions, diffractively excited meson resonances and, finally, the continuum diffractive states. Although the quark-antiquark interaction in the $q\bar{q}$ Fock states of elastic pions and diffractive meson resonances is important for the formation of pions and its excitations, the contribution to their wave function from large invariant mass, $M_{q\bar{q}}$, Fock states vanishes rapidly at very large $M_{q\bar{q}}$. Then, as argued in [11], the FS interaction between the FS quark and antiquark can be neglected and the $q\bar{q}$ plane-wave approximation becomes applicable as soon as the invariant mass of the forward dijet system exceeds a typical mass scale of prominent meson resonances. Consequently, the technique of section 3 and the derivation of a nonlinear nuclear $k_\perp$-factorization in section 4 are fully applicable to breakup of pions into high-mass hard dijets.

4.2. In-volume breakup is hard pQCD tractable, probes the pion distribution amplitude but is subleading at large $\boldsymbol{p}_\pm$

Whether the breakup of non-pointlike pions into hard dijets, $\boldsymbol{p}_\pm^2 \gtrsim Q_A^2$, is under full control of perturbative QCD or not needs further scrutiny. In the case of DIS it was important that the wave function of the photon was a slow function compared to nuclear WW glue, see the discussion preceding the derivation of eq. (51) in section 4. Here we notice that for extended heavy nuclei the saturation scale Q_A is much larger than the (z-dependent) intrinsic transverse momentum of quarks, Q_π, in the pion, so that the pion wave function would be the steepest function of transverse momentum in the problem. A closer inspection of the nonlinear $k_\perp$-factorization formula (48) shows that one must compare the momentum dependence of the pion WF $\langle \pi | \boldsymbol{\kappa} \rangle$ with that of $\Phi((1-\beta)\nu_A(\boldsymbol{b}), \boldsymbol{\kappa})$ and or $\Phi(\beta\nu_A(\boldsymbol{b}), \boldsymbol{\kappa})$, i.e, Q_π^2 must be compared to the β-dependent saturation scale $Q_\beta^2 = \beta Q_A^2$ or $(1-\beta)Q_A^2$.

We shall consider first the contribution to the dijet cross section from $Q_\beta^2 \gtrsim Q_\pi^2$, i.e., $\beta_{min} = Q_\pi / Q_A^2 \lesssim \beta \lesssim \beta_{\max} = 1 - \beta_{min}$. It describes the in-volume breakup of pions, see the interpretation of eq. (37). Here the pion WF is the steepest one compared to other factors in (48) and can be approximated by a δ-function in transverse momentum space ,

$$\langle z,\boldsymbol{p}|\pi\rangle = (2\pi)^2\delta(\boldsymbol{p})\int \frac{d^2\boldsymbol{k}}{(2\pi)^2}\langle z,\boldsymbol{k}|\pi\rangle = (2\pi)^2\delta(\boldsymbol{p})\sqrt{\frac{\pi}{2N_c}}F_\pi\varphi_\pi(Q^2_\beta,z)\,, \qquad (53)$$

which gives

$$\frac{1}{(2\pi)^2}\int d^2\boldsymbol{\kappa}_1\Phi((1-\beta)\nu_A(\boldsymbol{b}),\boldsymbol{\kappa}_1)\left\{\langle z,\boldsymbol{p}_-+\boldsymbol{\kappa}_1+\boldsymbol{\kappa}_3|\pi\rangle - \langle z,\boldsymbol{p}_-+\boldsymbol{\kappa}_1+\boldsymbol{\kappa}_3+\boldsymbol{\kappa}|\pi\rangle\right\}$$
$$\approx\sqrt{\frac{\pi}{2N_c}}F_\pi\varphi_\pi(Q^2_\beta,z)[\Phi((1-\beta)\nu_A(\boldsymbol{b}),\boldsymbol{p}_-+\boldsymbol{\kappa}_3)-\Phi((1-\beta)\nu_A(\boldsymbol{b}),\boldsymbol{p}_-+\boldsymbol{\kappa}_3+\boldsymbol{\kappa})]\,, \qquad (54)$$

where we indicated explicitly the factorization scale Q^2_β in the πDA $\varphi_\pi(Q^2_\beta,z)$. Of the two possible helicity structures in (13) only the one, $\propto\delta_{\lambda-\bar{\lambda}}$, related to the pion decay constant, contributes in this hard regime, see also the related discussion of diffractive dijets in [11]. Then this contribution to the breakup of pions into high-mass dijets can be presented in two equivalent forms, which only differ by a reshuffling of the large jet momentum $\boldsymbol{p}_-$ between different factors in the integrand:

$$\begin{aligned}
\frac{d\sigma_\pi}{d^2\boldsymbol{b}dzd^2\boldsymbol{p}_-d^2\boldsymbol{\Delta}} &= \frac{\pi^3}{N_c}\cdot\alpha_S\sigma_0(x)T(\boldsymbol{b})F^2_\pi\\
&\times\int_{\beta_{min}}^{\beta_{max}}d\beta\varphi^2_\pi(Q^2_\beta,z)\int d^2\boldsymbol{\kappa}_3d^2\boldsymbol{\kappa}f(\boldsymbol{\kappa})\Phi(\beta\nu_A(\boldsymbol{b}),\boldsymbol{\Delta}-\boldsymbol{\kappa}_3-\boldsymbol{\kappa})\Phi(\beta\nu_A(\boldsymbol{b}),\boldsymbol{\kappa}_3)\\
&\times[\Phi((1-\beta)\nu_A(\boldsymbol{b}),\boldsymbol{p}_-+\boldsymbol{\kappa}_3)-\Phi((1-\beta)\nu_A(\boldsymbol{b}),\boldsymbol{p}_-+\boldsymbol{\kappa}_3+\boldsymbol{\kappa})]^2\\
&=\frac{\pi^3}{N_c}\cdot\alpha_S\sigma_0(x)T(\boldsymbol{b})F^2_\pi\\
&\times\int_{\beta_{min}}^{\beta_{max}}d\beta\varphi^2_\pi(Q^2_\beta,z)\int d^2\boldsymbol{q}d^2\boldsymbol{\kappa}f(\boldsymbol{\kappa})\Phi(\beta\nu_A(\boldsymbol{b}),\boldsymbol{p}_+-\boldsymbol{q}-\boldsymbol{\kappa})\Phi(\beta\nu_A(\boldsymbol{b}),\boldsymbol{p}_-+\boldsymbol{q})\\
&\times[\Phi((1-\beta)\nu_A(\boldsymbol{b}),\boldsymbol{q})-\Phi((1-\beta)\nu_A(\boldsymbol{b}),\boldsymbol{q}+\boldsymbol{\kappa})]^2\,. \qquad (55)
\end{aligned}$$

Alternatively, one could have neglected the $\boldsymbol{r}$-dependence of the pion wave function, i.e., put the radial WF $\Psi_\pi(z,\boldsymbol{r})\approx\Psi_\pi(z,0)$ and proceed with the calculations which lead to (48).

At first sight, in close similarity to the breakup into coherent diffractive dijets [11], the inclusive dijet cross section is proportional to the πDA squared. One must be careful with the isolation of the leading large-$\boldsymbol{p}_\pm$ behavior of the pion breakup, though.

Consider first the former representation of (55) According to [11, 26], in the hard region $f(\boldsymbol{\kappa})\sim 1/(\boldsymbol{\kappa}^2)^\delta$ with the exponent $\delta\sim 2$ and $\Phi(\nu_A(\boldsymbol{b}),\boldsymbol{\kappa})\approx\nu_A(\boldsymbol{b})f(\boldsymbol{\kappa})$, see eq. (44), so that it is tempting to focus on $\boldsymbol{\kappa}_3^2\lesssim\beta Q^2_A$ and neglect $\boldsymbol{\kappa}_3$ compared to $\boldsymbol{p}_-$ in (54):

$$[\Phi((1-\beta)\nu_A(\boldsymbol{b}),\boldsymbol{p}_--\boldsymbol{\kappa}_3)-\Phi((1-\beta)\nu_A(\boldsymbol{b}),\boldsymbol{p}_--\boldsymbol{\kappa}_3-\boldsymbol{\kappa})]^2$$
$$\approx[\Phi((1-\beta)\nu_A(\boldsymbol{b}),\boldsymbol{p}_-)-\Phi((1-\beta)\nu_A(\boldsymbol{b}),\boldsymbol{p}_--\boldsymbol{\kappa})]^2\,. \qquad (56)$$

Upon taking the convolution (50), this contribution to the dijet cross section can be cast into a form reminiscent of (51):

$$\frac{d\sigma_\pi}{d^2\boldsymbol{b}dzd^2\boldsymbol{p}_-d^2\boldsymbol{\Delta}} = T(\boldsymbol{b})\int_0^{\beta_{max}} d\beta \int d^2\boldsymbol{\kappa}\Phi(2\beta\nu_A(\boldsymbol{b}),\boldsymbol{\Delta}-\boldsymbol{\kappa})\frac{d\sigma_{eff}}{dzd^2\boldsymbol{p}_+d^2\boldsymbol{\kappa}}\,, \tag{57}$$

where

$$\begin{aligned}\frac{d\sigma_{eff}}{dzd^2\boldsymbol{p}_+d^2\boldsymbol{\kappa}} &= \frac{1}{2(2\pi)^2}\cdot\frac{\pi}{2N_c}\cdot\alpha_S\sigma_0(x)F_\pi^2\varphi_\pi^2(Q_\beta^2,z)f(\boldsymbol{\kappa})\\ &\times\ [\Phi((1-\beta)\nu_A(\boldsymbol{b}),\boldsymbol{p}_-)-\Phi((1-\beta)\nu_A(\boldsymbol{b}),\boldsymbol{p}_--\boldsymbol{\kappa})]^2\end{aligned} \tag{58}$$

plays the rôle of the free-nucleon cross section for DIS, eq. (5) and $\Phi((1-\beta)\nu_A(\boldsymbol{b}),\boldsymbol{p})$ emerges as the counterpart of the WF $\langle\boldsymbol{p}|\gamma^*\rangle$ in (5), (51). Now we notice that this consideration is fully applicable to $\beta<\beta_{min}$, for which reason we already have put $\beta=0$ for the lower limit of the β integration in (57).

The nuclear WW gluon distribution $\Phi(2\beta\nu_A(\boldsymbol{b}),\boldsymbol{\Delta}-\boldsymbol{\kappa})$ in (57) provides a cutoff of the $\boldsymbol{\kappa}$ integration, $\boldsymbol{\kappa}^2\lesssim\beta Q_A^2+\boldsymbol{\Delta}^2$, which justifies the small-κ approximation

$$\begin{aligned}&[\Phi((1-\beta)\nu_A(\boldsymbol{b}),\boldsymbol{p}_-)-\Phi((1-\beta)\nu_A(\boldsymbol{b}),\boldsymbol{p}_--\boldsymbol{\kappa})]^2\\ &\qquad\approx 2\left(\frac{f(\boldsymbol{p}_-)}{\boldsymbol{p}_-^2}\right)^2\delta^2(1-\beta)^2\nu_A^2(\boldsymbol{b})\boldsymbol{p}_-^2\boldsymbol{\kappa}^2\,,\end{aligned} \tag{59}$$

where the azimuthal averaging has been performed. Then the $\boldsymbol{\kappa}$ integration subject to $\boldsymbol{\kappa}^2\lesssim\beta Q_A^2+\boldsymbol{\Delta}^2$ yields

$$\int d^2\boldsymbol{\kappa}f(\boldsymbol{\kappa})\boldsymbol{\kappa}^2\approx\frac{4\pi^2}{\sigma_0(x)N_c}G(\boldsymbol{\Delta}^2+\beta Q_A^2) \tag{60}$$

and the final results for this contribution to the dijet cross section reads

$$\begin{aligned}\left.\frac{d\sigma_{\pi A}^{(volume)}}{d^2\boldsymbol{b}dzd^2\boldsymbol{p}_-d^2\boldsymbol{\Delta}}\right|_{hard} &\approx \frac{32\pi^6F_\pi^2T^3(\boldsymbol{b})}{N_c^4}\cdot\frac{\delta^2\alpha_S^3(\boldsymbol{p}_-^2)\mathcal{F}^2(x,\boldsymbol{p}_-^2)}{(\boldsymbol{p}_-^2)^5}\cdot\\ &\times\int_0^1 d\beta(1-\beta)^2\varphi_\pi^2(Q_\beta^2,z)\Phi(2\beta\nu_A(\boldsymbol{b}),\boldsymbol{\Delta})G(\boldsymbol{\Delta}^2+\beta Q_A^2)\,.\end{aligned} \tag{61}$$

Here the β integration is dominated by the mid-β contribution, hence the β integration can safely be extended from 0 to 1. The dominance of the mid-β contribution means that the incident pion breaks in the volume of a nucleus, i.e., it selects weakly attenuating small color-dipole configurations in the incident pion. For this reason it is uniquely calculable in terms of hard quantities and collective nuclear WW glue, the auxiliary soft parameter $\sigma_0(x)$ does not enter (61), hence the subscript "hard" in the l.h.s. of (61). All the approximations which have lead to the proportionality of the pion breakup cross section to the πDA squared were indeed well justified. Unfortunately, as far as the p_+ dependence is concerned the in-volume hard absorption gives the subleading, higher-twist contribution.

4.3. The leading asymptotics at large $\boldsymbol{p}_\pm$ is dominated by soft absorption on the front face of a nucleus

The leading asymptotics at large $\boldsymbol{p}_\pm$ can be isolated starting with the latter representation of eq. (55). It comes from $|\boldsymbol{q}| = |\boldsymbol{p}_- - \boldsymbol{\kappa}_3| \ll Q_A$, furthermore, as we shall see a posteriori the dominant contribution comes from a still narrower soft domain $|\boldsymbol{q}| \lesssim Q_\pi$. We start with the in-volume contribution from $\beta_{min} < \beta < 1 - \beta_{min}$. According to (44), for such hard jets we can approximate

$$\Phi(\beta\nu_A(\boldsymbol{b}), \boldsymbol{p}_+ - \boldsymbol{q} - \boldsymbol{\kappa})\Phi(\beta\nu_A(\boldsymbol{b}), \boldsymbol{p}_- + \boldsymbol{q}) \approx \beta^2\nu_A^2(\boldsymbol{b})f(\boldsymbol{p}_+)f(\boldsymbol{p}_-)\,. \tag{62}$$

Now, using the convolution identity eq.(50), we may simplify

$$\begin{aligned}
&\int d^2\boldsymbol{q}d^2\boldsymbol{\kappa}f(\boldsymbol{\kappa})[\Phi((1-\beta)\nu_A(\boldsymbol{b}), \boldsymbol{q}) - \Phi((1-\beta)\nu_A(\boldsymbol{b}), \boldsymbol{q}+\boldsymbol{\kappa})]^2 = \\
&= 2\int d^2\boldsymbol{\kappa}f(\boldsymbol{\kappa})[\Phi(2(1-\beta)\nu_A(\boldsymbol{b}), \boldsymbol{0}) - \Phi(2(1-\beta)\nu_A(\boldsymbol{b}), \boldsymbol{\kappa})] \\
&= -2\int d^2\boldsymbol{\kappa}f(\boldsymbol{\kappa})\,\frac{\partial\Phi(2(1-\beta)\nu_A(\boldsymbol{b}), \boldsymbol{\kappa}^2)}{\partial\boldsymbol{\kappa}^2}\Big|_{\boldsymbol{\kappa}^2=0}\cdot\boldsymbol{\kappa}^2 \\
&\simeq \frac{4\pi}{(1-\beta)^2}\cdot\frac{1}{Q_A^4}\cdot\frac{1}{\sigma_0(x)N_c}\cdot G(Q_\beta^2)\,.
\end{aligned} \tag{63}$$

where $Q_\beta^2 = (1-\beta)Q_A^2$ and we made explicit use of the parametrization (45). The singular behaviour at $\beta \to 1$ shows that the inclusive cross section will be dominated by the soft end-point contribution from $Q_\beta^2 \sim Q_\pi^2$,

$$\int_{\beta_{min}}^{\beta_{max}} \frac{d\beta G(Q_\beta^2)\beta^2\varphi_\pi^2(Q_\beta^2, z)}{(1-\beta)^2} \sim \frac{G(Q_\pi^2)\varphi_\pi^2(Q_\pi^2, z)}{1-\beta_{\max}} = \frac{Q_A^2}{Q_\pi^2}\cdot G(Q_\pi^2)\varphi_\pi^2(Q_\pi^2, z)\,, \tag{64}$$

i.e., the in-volume contribution is squeezed to the breakup of pions close to the front face of the nucleus. Finally, making use of (46) and neglecting the difference between $G(Q_\pi^2)$ and $G(Q_A^2)$, we obtain an estimate

$$\frac{d\sigma_{\pi A}^{(soft)}}{d^2\boldsymbol{b}dzd^2\boldsymbol{p}_-d^2\boldsymbol{p}_+} = \frac{4\pi^4T^2(\boldsymbol{b})\alpha_S^2(\boldsymbol{p}_\pm^2)F_\pi^2}{N_c^3}\cdot\phi_\pi^2(Q_\pi^2, z)\cdot\frac{1}{Q_\pi^2}\cdot\frac{\mathcal{F}(x, \boldsymbol{p}_+^2)}{(\boldsymbol{p}_+^2)^2}\cdot\frac{\mathcal{F}(x, \boldsymbol{p}_-^2)}{(\boldsymbol{p}_-^2)^2}\,. \tag{65}$$

The striking feature of this result is a complete decorrelation of the two jets. For the explanation of the superscript "soft" see below.

In the evaluation of the contribution from $\beta_{\max} \lesssim \beta \lesssim 1$, i.e., from breakup of pions on the front face of the nucleus, we can take $\Phi((1-\beta)\nu_A(\boldsymbol{b}),\boldsymbol{\kappa}_1) = \delta(\boldsymbol{\kappa}_1)$, see eq. (40), so that for hard dijets

$$\begin{aligned}&\int d^2\boldsymbol{\kappa}_1 \Phi((1-\beta)\nu_A(\boldsymbol{b}),\boldsymbol{\kappa}_1)\left\{\langle\pi|z,\boldsymbol{p}_- + \boldsymbol{\kappa}_1 + \boldsymbol{\kappa}_3\rangle - \langle\pi|z,\boldsymbol{p}_- + \boldsymbol{\kappa}_1 + \boldsymbol{\kappa}_3 + \boldsymbol{\kappa}\rangle\right\} \\ &\approx \langle\pi|z,\boldsymbol{p}_- + \boldsymbol{\kappa}_3\rangle - \langle\pi|z,\boldsymbol{p}_- + \boldsymbol{\kappa}_3 + \boldsymbol{\kappa}\rangle \end{aligned} \tag{66}$$

Putting $\beta = 1$ in the rest of the integrand of (48), approximating $\int_{\beta_{max}}^1 d\beta \sim Q_\pi^2/Q_A^2$, and reshuffling $\boldsymbol{p}_-$ as in (55) we obtain

$$\begin{aligned}\frac{d\sigma_\pi^{surface}}{d^2\boldsymbol{b}dzd^2\boldsymbol{p}_-d^2\boldsymbol{\Delta}} &\approx \frac{1}{2(2\pi)^2 Q_A^2}\cdot\alpha_S\sigma_0(x)T(\boldsymbol{b})\Phi(\nu_A(\boldsymbol{b}),\boldsymbol{p}_+)\Phi(\nu_A(\boldsymbol{b}),\boldsymbol{p}_-) \\ &\times\; Q_\pi^2\int d^2\boldsymbol{q}d^2\boldsymbol{\kappa} f(\boldsymbol{\kappa})\left|\langle\pi|z,\boldsymbol{q}\rangle - \langle\pi|z,\boldsymbol{q}+\boldsymbol{\kappa}\rangle\right|^2 , \end{aligned} \tag{67}$$

Although $f(\boldsymbol{\kappa})$ and the pion WF are distributions of comparable width, for the estimation purposes we can expand

$$\left|\langle\pi|z,\boldsymbol{q}\rangle - \langle\pi|z,\boldsymbol{q}+\boldsymbol{\kappa}\rangle\right|^2 \sim \frac{\left|\langle\pi|z,\boldsymbol{q}\rangle\right|^2}{(Q_\pi^2+\boldsymbol{q}^2)^2} 2\boldsymbol{q}^2\boldsymbol{\kappa}^2 . \tag{68}$$

The $\boldsymbol{\kappa}$ integration will yield $G(Q_\pi^2+\boldsymbol{q}^2) \sim G(Q_\pi^2)$, see eq. (60), whereas

$$2Q_\pi^2 \int d^2\boldsymbol{q}\frac{\left|\langle\pi|z,\boldsymbol{q}\rangle\right|^2\boldsymbol{q}^2}{(Q_\pi^2+\boldsymbol{q}^2)^2} \sim \frac{1}{\pi Q_\pi^2}\left|\int d^2\boldsymbol{q}\langle\pi|z,\boldsymbol{q}\rangle\right|^2 \sim \frac{(2\pi)^4}{Q_\pi^2}\cdot\frac{1}{2N_c}F_\pi^2\varphi_\pi^2(Q_\pi^2,z) . \tag{69}$$

Notice, that both helicity components of the pion WF would contribute in this soft regime. Then, our result for (67) is identical to (65), so that the final estimate for the soft cross section is (65) times a factor ~ 2.

Several comments on our result (65), (67) are in order. First, the representation (38) for the distortion factor entails that the dominance by the contribution from $\beta \to 1$ corresponds to an absorption of the pion in the state with normal hadronic size on the front surface of the nucleus, i.e., it is a soft absorption driven contribution to excitation of hard dijets, hence the superscript "soft" in the l.h.s. of (65). Second, the same point about absorbed pions being in the state with large hadronic size is manifest from the emergence of the soft factor $1/Q_\pi^2$ in the dijet cross section. Third, the back-to-back correlated hard contribution (61) is suppressed compared to the soft contribution (65), (67) by a factor $1/\boldsymbol{p}_\pm^2$, i.e., it has the form of a higher twist correction. Fourth, as far as the dependence on transverse momentum is concerned the dijet cross section from the soft absorption mechanism has the form of a product of two single-jet cross sections (12). This property indicates that hard jets acquire their large transverse momenta from hard scattering on different nucleons which explains why the transverse momenta of the quark and antiquark are fully decorrelated both azimuthally and longitudinally, i.e., in the magnitude of the momenta $|\boldsymbol{p}_+|$ and $|\boldsymbol{p}_-|$ (in the scattering plane). This must be contrasted to the breakup of photons when the large momentum of jets comes from the intrinsic momentum in the photon WF and jets are produced predominantly back-to-back with the scale for both the azimuthal (out-of-plane) and longitudinal (in-plane) decorrelations being set by Q_A. Consequently, the out-of-plane decorrelation momentum in the breakup of pions into forward dijets is predicted to be much larger than in the breakup of photons in photoproduction or DIS.

4.4. Transverse energy associated with dijets in the photon and pion breakup

There is still another interesting difference between the breakup of pointlike photons and non-pointlike pions. It is the surplus transverse energy of secondary particles associated with the forward hard jets.

What counterbalances the large transverse momenta $\boldsymbol{p}_\pm$ of the two uncorrelated hard jets? According to [6, 11], the hard tail (44) of the collective nuclear WW glue which enters (62) is dominated by a single hard gluon. Then in the pQCD Born approximation the forward $q, \bar{q}$ hard jets would recoil against the valence quarks of nucleons of the target nucleus. With allowance for the QCD evolution effects the recoil is against the mid-rapidity gluons and quarks, which are separated from the forward hard dijets by at least several units of rapidity. Although the partons which counterbalance the forward dijets are not localized in the rapidity, their overall contribution to the transverse energy production in an event (with the transverse energy from forward dijets excluded) will be an amount of $\Delta E_T \sim |\boldsymbol{p}_+|+|\boldsymbol{p}_-|$ in excess of the average transverse energy in a minimal bias event without hard forward jets. This surplus transverse energy production ΔE_T would not depend on the azimuthal angle between the two jets.

In the breakup of photons the surplus transverse energy ΔE_T will be much smaller. Indeed, the large transverse momenta of jets come from the large intrinsic transverse momentum of the quark and antiquark in the photon. The dijet recoils against other secondary particles with a transverse momentum which is precisely equal to the acoplanarity momentum $|\boldsymbol{\Delta}|$. The strong decorrelation, $\boldsymbol{\Delta}^2 \gtrsim Q_A^2$, is driven by exchange of one hard gluon, see the discussion of (44), and we expect a surplus transverse energy $\Delta E_T \approx |\boldsymbol{\Delta}|$. In the back-to-back configuration, $\boldsymbol{\Delta}^2 \lesssim Q_A^2$, the nuclear glue $\Phi(\nu_A(\boldsymbol{b}), \boldsymbol{\Delta})$ is a result of the fusion of $\propto A^{1/3}$ soft gluons, and we expect the surplus transverse energy $\Delta E_T \approx Q_A$.

4.5. Is the pion distribution amplitude measurable in the pion breakup into dijets?

The emergence of the z-dependent soft factor $1/Q_\pi^2$ in (65), which depends on the model for soft wave function of the pion, (see also the analysis (67)-(69)), is an unfortunate circumstance. It makes the relationship between the z-dependence of the dijet cross section and the πDA squared a model dependent one. Still, the experimental isolation of the hard component (61) and thereby the measurement of the πDA is not an entirely impossible task.

The point is that the hard component (61) from the in-volume breakup gives rise to back-to-back jets within a small angular cone limited by the decorrelation momentum $\boldsymbol{\Delta}^2 \lesssim Q_A^2$. In the $\boldsymbol{\Delta}$-plane it is a well defined peak. Consequently, although the z-dependence of Q_π^2 is not under good theoretical control, it can be determined experimentally measuring the dijet cross section beyond the back-to-back cone. Then the soft contribution can reliably be extrapolated into the back-to-back cone and the observed excess signal can be identified with the hard contribution. Approximating the hard cross section at $\boldsymbol{\Delta} \sim 0$ by the integrand of (61) at $\beta \sim 1/2$ and comparing it to the soft cross section (65) times the above estimated factor of three to four, we find

$$\frac{d\sigma^{(hard)}}{d\sigma^{(soft)}} \sim \delta^2 \frac{Q_\pi^2}{\pi \boldsymbol{p}_+^2} \tag{70}$$

As an example of the model estimate [11] for the pion WF which reproduces the pion electromagnetic form factor, the $\pi^0 \to 2\gamma$ decay width and the form factor of $\gamma^*\gamma\pi$ transition, we cite $Q_\pi^2 \sim 0.17$ GeV^2. The extraction of the small hard signal is facilitated by its specific dependence on $\boldsymbol{\Delta}$.

4.6. *Dijets for the power-law wave function of the pion*

Above we saw how substantially the dijet cross section changes from the pointlike photon to the non-pointlike pion with the limited intrinsic transverse momentum of the quark and antiquark in the pion. It is interesting to see how our main conclusions for the pion breakup will change – if at all – for a power-law wave function of the form

$$\langle z, \boldsymbol{p}|\pi\rangle \propto (2\pi)^2 F_\pi \varphi(z)\sqrt{\frac{\pi}{2N_c}} \cdot \frac{1}{\pi} \cdot \frac{Q_\pi^2}{(\boldsymbol{p}^2 + Q_\pi^2)^2}\,. \tag{71}$$

A detailed discussion of properties of the pion for such a dipole, Coulomb-like, WF and its applications to the pion form factor and forward and non-forward parton distributions in the pion is found in [39], an early discussion of some of these issues for the power-law WF of the proton is found in [24]. A simple choice [24, 40, 41] suggested by the relativization of Coulomb-like wave functions is $Q_\pi^2 = z(1-z)\Lambda_\pi^2 + m_f^2$, cf. eq. (8) for the photon, for a slightly different parameterization see [39]. The dipole WF can be regarded as a minimal non-pointlike departure from the pointlike pion which would correspond to a monopole wave function, cf. eq. (7).

For the purposes of our discussion, the dipole wave function has the same asymptotics at large transverse momenta as the unintegrated nuclear glue (45). Consequently, following the discussion in [6, 7] the convolution (54) can be evaluated as

$$\begin{aligned}
&\frac{1}{(2\pi)^2}\int d^2\boldsymbol{\kappa}_1 \Phi((1-\beta)\nu_A(\boldsymbol{b}), \boldsymbol{\kappa}_1)\left\{\langle\pi|z, \boldsymbol{p}_- + \boldsymbol{\kappa}_1 + \boldsymbol{\kappa}_3\rangle - \langle\pi|z, \boldsymbol{p}_- + \boldsymbol{\kappa}_1 + \boldsymbol{\kappa}_3 + \boldsymbol{\kappa}\rangle\right\} \\
&\quad \approx \sqrt{\frac{\pi}{2N_c}} F_\pi \varphi_\pi(Q_\beta^2, z)[\tilde{\Phi}(Q_\beta^2(\boldsymbol{b}) + Q_\pi^2, \boldsymbol{p}_- + \boldsymbol{\kappa}_3) - \tilde{\Phi}(Q_\beta^2(\boldsymbol{b}) + Q_\pi^2, \boldsymbol{p}_- + \boldsymbol{\kappa}_3 + \boldsymbol{\kappa})]
\end{aligned} \tag{72}$$

where $\tilde{\Phi}(Q_\beta^2(\boldsymbol{b}) + Q_\pi^2, \boldsymbol{\kappa})$ is described by the parameterization (45) subject to the substitution

$$Q_A^2 \to Q_\beta^2(\boldsymbol{b}) + Q_\pi^2\,. \tag{73}$$

The separation of the leading large-$\boldsymbol{p}_\pm$ asymptotics and isolation of the hard contribution for the dipole Ansatz fully corroborates the main conclusions of sections 5.2 and 5.3 on the dominance of the in-volume contribution to the back-to-back correlated hard dijets and the surface breakup contribution into uncorrelated dijets. The model dependence enters through Q_π^2 in (73) and can be neglected at large β, i.e., for the in-volume breakup of pions. However, the model dependent Q_π^2 would dominate (73) for breakup on the front surface of the nucleus.

SUMMARY AND CONCLUSIONS

We presented a comparison of consequences of the nuclear $k_\perp$-factorization for the breakup of non-pointlike pions and pointlike photons into forward dijets. In striking contrast to the pQCD tractable hard breakup of photons, the dominant contribution to the breakup of pions starts from the soft breakup of pions into quark and antiquark at the front face of the target nucleus followed by hard intranuclear rescattering of the quark and antiquark. The most striking prediction is a complete azimuthal decorrelation of hard jets in the breakup of pions. An obvious implication is that the out-of-plane dijet decorrelation momentum squared $\langle\Delta_T^2\rangle_{\pi A}$ in the breakup of pions must be much larger than $\langle\Delta_T^2\rangle_{\gamma A}$ in the breakup of photons.

A direct comparison of the A-dependence of photo- and pion-produced dijets at $\sqrt{s} = 21$ GeV has been performed in the E683 Fermi-lab experiment [42] and gave a solid evidence for $\langle\Delta_T^2\rangle_{\pi A} > \langle\Delta_T^2\rangle_{\gamma A}$. Unfortunately, these data are on mid-rapidity jets at relatively large values of $x \gtrsim x_A$, beyond the applicability of the concept of fusion of partons. Coherent diffractive forward dijets have been observed at Fermi-lab by the E791 collaboration [43]. The experimental identification of diffractive dijets in the E791 experiment has been facilitated by their exact back-to-back property, $\mathbf{\Delta}^2 \lesssim 1/R_A^2$. A similar identification of forward dijets from the breakup of pions in inelastic πA collisions might be problematic, but our principal prediction of $\langle\Delta_T^2\rangle_{\pi A} > \langle\Delta_T^2\rangle_{\gamma A}$ can be tested even under the most liberal event selection criteria.

Specifically, one only needs to study the azimuthal distribution properties of the hadronic subsystem in the first several units of the forward rapidity. For instance, one can define on an event-by-event basis the two-dimensional analogs of the familiar thrust and sphericity variables (for the review see [44]). Then we predict that the forward system in πA interactions will be more spherical than in γA interactions, and the 2D thrust for γA with be larger than for πA. Such an analysis can be performed also in the COMPASS experiment at CERN in which the forward systems produced by photons and pions can be studied in the same apparatus [16]. Still another observable which differentiates between the breakup of pointlike photons and non-pointlike pions is a surplus transverse energy of secondary particles associated with forward hard jets - for the same transverse momenta of jets it is larger in πA than in γA collisions.

The experimental isolation of the higher-twist back-to-back correlated hard contribution from the in-volume breakup is feasible and would allow the determination of the pion distribution amplitude. This challenging task can be accomplished because the background from decorrelated dijets can be determined experimentally and the back-to-back contribution has a specific dependence on the decorrelation momentum which broadens with the target mass number.

The breakup of pions into hard dijets involves the stage of soft absorption at the front face of the target nucleus and the cross section is sensitive to models of the pion wave function. Nonetheless, the predicted transverse momentum dependence of pionic dijets does not change from soft models with a strong bound on the intrinsic momentum of quarks in the pion to modern semihard, power-law (dipole) wave functions.

We are glad to contribute to the Yu.A. Simonov Festschrift. One of the authors (NNN) recalls vividly from his student years, late 60's, how much I.S. Shapiro, then the leader of the Nuclear Theory Group, praised Simonov's work on the hyperspherical approach to many–body systems, the subject of Yurii Antonovich's habilitation thesis. Ever since then Yurii Antonovich remained at the forefront of hadron physics and non-perturbative QCD and we take this occasion to wish Yurii Antonovich to keep his vigour and creativity.

This work has been partly supported by the INTAS grant 00-00366 and the DFG grant 436RUS17/72/03

1. E. Leader and E. Predazzi, *Introduction to Gauge Theories and Modern Particle Physics, v.1*, Cambridge University Press, Cambridge, 1996; G. Sterman, *An Introduction to Quantum Field Theory*, Cambridge University Press, Cambridge, 1993.
2. A.H. Mueller, Nucl. Phys. B **335** (1990) 115.
3. A.H. Mueller, Nucl. Phys. B **558** (1999) 285; in *QCD PERSPECTIVES ON HOT AND DENSE MATTER: Proceedings.* Edited by J.-P. Blaizot and E. Iancu. Dordrecht, The Netherlands, Kluwer, (2002) (NATO Science Series, II, Mathematics, Physics, and Chemistry, Vol. 87), pp. 45-72, [arXiv: hep-ph/0111244].
4. L. McLerran and R. Venugopalan, Phys. Rev. D **49** (1994) 2233; J.Jalilian-Marian, A. Kovner, L.D. McLerran and H. Weigert, Phys. Rev. D **55** (1997) 5414; E. Iancu, A. Leonidov and L. McLerran, in *QCD PERSPECTIVES ON HOT AND DENSE MATTER: Proceedings.* Edited by J.-P. Blaizot and E. Iancu. Dordrecht, The Netherlands, Kluwer, (2002) (NATO Science Series, II, Mathematics, Physics, and Chemistry, Vol. 87), pp. 73-145, [arXiv: hep-ph/0202270].
5. N.N. Nikolaev, W. Schäfer, B.G. Zakharov and V.R. Zoller, JETP Lett. **76** (2002) 195 [Pisma Zh. Eksp. Teor. Fiz. **76** (2002) 231]
6. N.N. Nikolaev, W. Schäfer, B.G. Zakharov and V.R. Zoller, J. Exp. Theor. Phys. **97** (2003) 441 [Zh. Eksp. Teor. Fiz. **124** (2003) 491]
7. I.P. Ivanov, N.N. Nikolaev, W. Schäfer, B.G. Zakharov and V.R. Zoller, Lectures on Diffraction and Saturation of Nuclear Partons in DIS off Heavy Nuclei, Proceedings of 36-th Annual Winter School on Nuclear and Particle Physics and 8-th St. Petersburg School on Theoretical Physics, St. Petersburg, Russia, 25 Feb - 3 Mar 2002. [arXiv: hep-ph/021216]; High Density QCD, Saturation and Diffractive DIS. Invited talk at the NATO Advanced Research Workshop on Diffraction 2002, Alushta, Ukraine, 31 Aug - 6 September 2002, [arXiv: hep-ph/0212176]; Diffractive Hard Dijets and Nuclear Parton Distributions, Proceedings of the Workshop on Exclusive Processes at High Momentum Transfer, Jefferson Lab, May 15-18, 2002. Editors A. Radyushkin and P. Stoler, World Scientific, 2002, pp. 205-213, [arXiv:hep-ph/0207045]; High Density QCD and Saturation of Nuclear Partons, Proceedings of the Conference on Quark Nuclear Physics (QNP'2002), June 9-14, Jülich, Germany, editors C. Elster, J. Speth and Th.

Walcher, Eur. Phys. J. A **18** (2003), 437 , [arXiv: hep-ph/0209298]; High Density QCD, Saturation and Diffractive DIS. Plenary talk at the International Symposium on Multiparticle Dynamics (ISMD'2002), Alushta, Ukraine, 8-14 September 2002, in *MULTIPARTICLE DYNAMICS: ISMD 2002: Proceedings.* Edited by A. Sissakian, G. Kozlov, E. Kolganova. River Edge, N.J., World Scientific, 2003, pp.209-220,[arXiv: hep-ph/0212176].

8. A. Szczurek, N.N. Nikolaev, W. Schäfer, and J. Speth, Phys. Lett. B **500** , 254 (2001)
9. J. R. Forshaw and R. G. Roberts, Phys. Lett. B **335**, 494 (1994); A. J. Askew, D. Graudenz, J. Kwiecinski and A. D. Martin, Phys. Lett. B **338**, 92 (1994); J. Kwiecinski, A. D. Martin and A. M. Stasto, Phys. Lett. B **459**, 644 (1999)
10. N.N. Nikolaev and V.I. Zakharov, Sov. J. Nucl. Phys. **21** (1975) 227; [Yad. Fiz. **21** (1975) 434]; Phys. Lett. B **55** (1975) 397.
11. N.N. Nikolaev, W. Schäfer and G. Schwiete, JETP Lett. **72** (2000) 583; [Pisma Zh. Eksp. Teor. Fiz. **72** (2000) 583]; Phys. Rev. D **63** (2001) 014020.
12. S. Frullani and J. Mougey, Adv. Nucl. Phys. **14**, 3 (1984).
13. V.L. Chernyak and A.R. Zhitnitsky, Phys. Rept. **112** (1984) 173; G.P. Lepage and S.J. Brodsky, Phys. Rev. D **22** (1980) 2157; S.J. Brodsky, H.-C. Pauli and S.S. Pinsky, Phys. Rept. **301** (1998) 299. R. Jakob and P. Kroll, Phys. Lett. B **315** (1993) 463; Erratum-ibid. B **319** (1993); A. P. Bakulev, S. V. Mikhailov and N. G. Stefanis, Phys. Lett. B **578** (2004) 91
14. V.M. Braun, D.Yu. Ivanov, A. Schäfer, L. Szymanowski, Phys. Lett. B **509** (2001) 43; Nucl. Phys. B **638** (2002) 111.
15. V.L. Chernyak, Phys. Lett. B **516** (2001) 116; V.L. Chernyak, A.G. Grozin, Phys. Lett. B **517** (2001) 119.
16. COMPASS. A Proposal for a COmmon Muon and Proton Apparatus for Structure and Spectroscopy. CERN/SPSLC 96-14, SPSLC/P297, 1 March 1996.
17. N.N. Nikolaev and B.G. Zakharov, Z. Phys. C **49** (1991) 607
18. N.N. Nikolaev and B.G. Zakharov, Z. Phys. C **53** (1992) 331.
19. N.N. Nikolaev and B.G. Zakharov, J. Exp. Theor. Phys. **78** (1994) 806; [Zh. Eksp. Teor. Fiz. **105** (1994) 1498]; Z. Phys. C **64** (1994) 631.
20. N.N. Nikolaev, B.G. Zakharov and V.R. Zoller, JETP Lett. **59** (1994) 6
21. N.N. Nikolaev and B.G. Zakharov. Phys. Lett. B **332** (1994) 184
22. N.N. Nikolaev, B.G. Zakharov and V.R. Zoller, Z. Phys. A **351** (1995) 435.

23. V. Barone, M. Genovese, N.N. Nikolaev, E. Predazzi and B.G. Zakharov, Phys. Lett. B **326** (1994) 161

24. V. Barone, M. Genovese, N.N. Nikolaev, E. Predazzi and B.G. Zakharov, Z. Phys. C **58** (1993) 541

25. L.N. Lipatov, Sov. J. Nucl. Phys **23** (1976) 338; E.A. Kuraev, L.N. Lipatov and V.S. Fadin, Sov. Phys. JETP **44** (1976) 443; **45** (1977) 199; Ya.Ya. Balitsky and L.N. Lipatov, Sov. J. Nucl. Phys **28** (1978) 822

26. I.P. Ivanov and N.N. Nikolaev, Phys. Atom. Nucl. **64**, 753 (2001), [Yad. Fiz. **64**, 813 (2001)]; Phys. Rev. D **65** 054004 (2002).

27. B. Andersson *et al.* (Small x Collab.), Eur. Phys. J. C **25**, 77 (2002)

28. T. Ahmed et al. (H1 Collab.), Nucl. Phys. B **445**, 195 (1995), and references therein.

29. N.N.Nikolaev and B.G.Zakharov, Phys. Lett. B **332** (1994) 177

30. M. Diehl, T. Feldmann, R. Jakob and P. Kroll, Eur. Phys. J. C **8** (1999) 409

31. A.V. Radyushkin, Phys. Rev. D**58** (1998) 114008

32. W. Jaus, Phys. Rev. D **44** (1991) 2851

33. Review of Particle Physics, Eur. Phys. J. C **3** (1998) 1

34. R. J. Glauber, in *Lectures in Theoretical Physics,* edited by W. E. Brittin et al. (Interscience Publishers, Inc., New York, 1959), Vol. 1, p. 315.

35. B.G. Zakharov, Sov. J. Nucl. Phys. **46** (1987) 92; [Yad. Fiz. **46** (1987) 148].

36. N.N. Nikolaev, G. Piller and B.G. Zakharov. J. Exp. Theor. Phys. **81** (1995) 851; Z. Phys. A **354** (1996) 99

37. B.G. Zakharov, JETP Lett. **63** (1996) 952; JETP Lett. **65** (1997) 615; Phys. Atom. Nucl. **61** (1998) 838;

38. C. Adler, et al. (STAR Collab.), Phys. Rev. Lett. **90**, 082302 (2003)

39. A. Mukherjee, I. V. Musatov, H. C. Pauli and A. V. Radyushkin, Phys. Rev. D **67** (2003) 073014.

40. M.V. Terentiev, Sov. J. Nucl. Phys. **24** 106 (1976); [Yad. Fiz. **24**, 207 (1976)]

41. J. Nemchik, N.N. Nikolaev and B.G. Zakharov, Phys. Lett. B **341**, 228 (1994); J. Nemchik, N.N. Nikolaev, E. Predazzi and B.G. Zakharov, Phys. Lett. B **374**, 199 (1996); Z. Phys. C **75**, 71 (1997)

42. D. Naples et al. (E683 Collab.), Phys. Rev. Lett. **72**, 2341 (1994)

43. E.M. Aitala et al. (E791 Collab.) Phys. Rev. Lett. **86**, 4768 (2001)

44. S.L. Wu, Phys. Rep. **107**, 59 (1984)

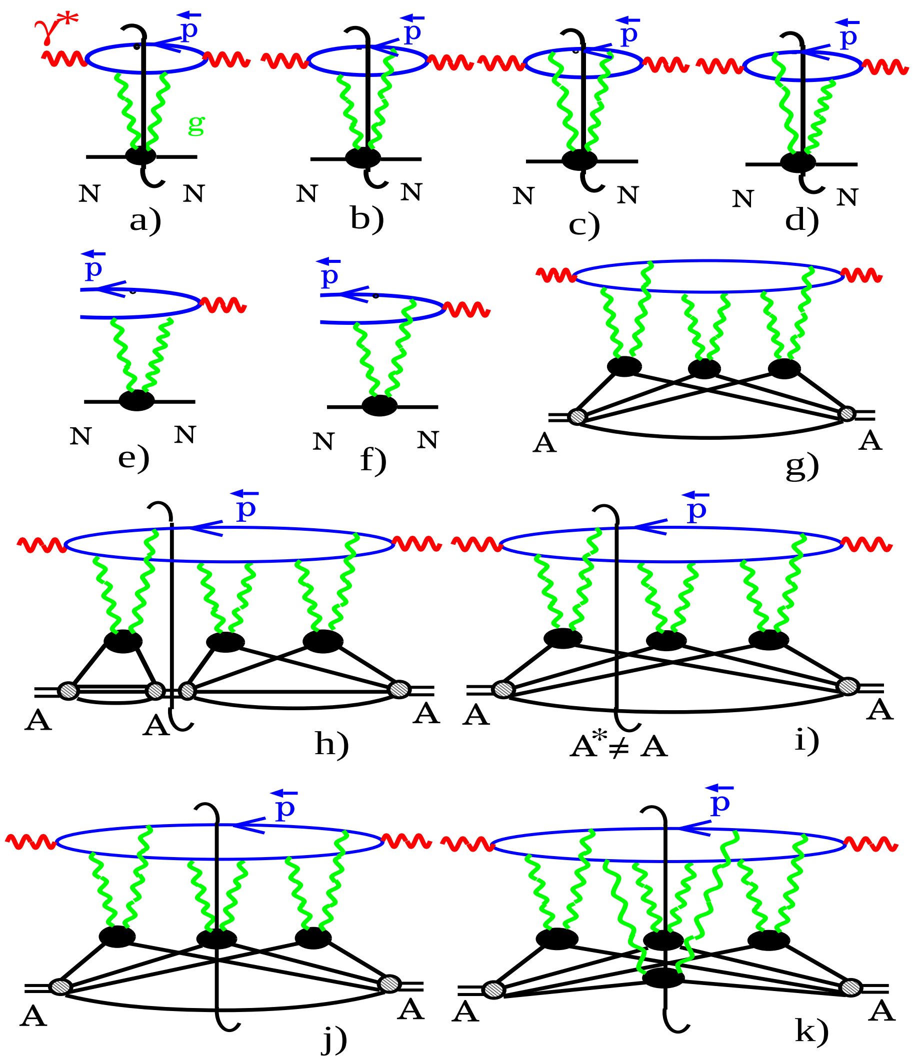

Figure 1. The pQCD diagrams for inclusive (a-d) and diffractive (e,f) DIS off protons and nuclei (g-k). Diagrams (a-d) show the unitarity cuts with color excitation of the target nucleon, (g) - a generic multiple scattering diagram for Compton scattering off nucleus, (h) - the unitarity cut for a coherent diffractive DIS, (i) - the unitarity cut for quasielastic diffractive DIS with excitation of the nucleus A^*, (j,k) - the unitarity cuts for truly inelastic DIS with single and multiple color excitation of nucleons of the nucleus.

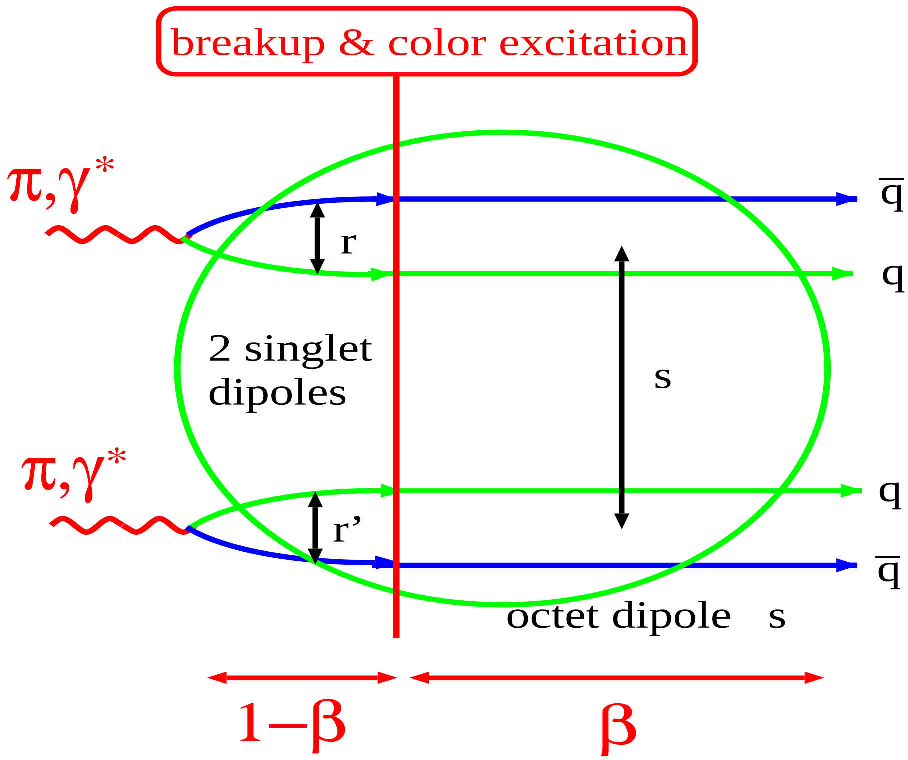

Figure 2. To the leading order the dijet system is excited into the color octet state on one nucleon after having travelled a fraction $1-\beta$ of the nucleus. After that an almost pointlike octet $q\bar{q}$–system travels the remaining fraction β.